

Responses to Reviewers

We thank you very much for your constructive comments and suggestions, which are very helpful to improve the scientific merits of this manuscript. We have carefully revised this manuscript according to your comments, and the amendments in the revised manuscript were presented in red font. Enclosed please find the point-by-point responses to the reviewers' comments. **This text in red is revision in the revised manuscript.** The line numbers in the response are from the revised manuscript.

Responses to Referee #2's comments

General comment: Chen et al. presents observations collected for ~1 month in a suburb of Beijing to investigate the sources of secondary aerosols, including secondary organic aerosol (SOA) and secondary inorganic aerosol (SIA). They suggest that higher SOA, total particulate matter (PM), and SIA increases with photochemical age, as determined by the ratio of toluene: benzene. The increase with photochemical age and correlation with ozone leads to a suggestion that SOA and SIA is controlled by photochemistry during this time period in the suburb.

Though of potential interest to the audience of ACP, similar to Reviewer #1, I have concerns about the methodology and interpretation of the data that needs to be addressed prior to being accepted and published into ACP. Also, many of the observations are not totally surprising due to studies from urban studies both in Beijing as well as around the world. Placing this study into the context of those studies, though, would add value, especially if a better contrast between suburban and urban chemistry

can be drawn through those comparisons.

The concerns/comments are below.

Response: Many thanks for your constructive comments and valuable suggestions, which would be much helpful to improve the scientific merits of this manuscript. The methodology and interpretation of the data have been carefully addressed in the revised manuscript. In the terms of methodology, to improve the reliability of photochemical age (t_a) as the surrogates of atmospheric oxidation capacity, 72 h back trajectories have been performed using the NOAA-HYSPLIT4 (HYbrid Single-Particle Lagrangian Integrated Trajectory) model, and a dominated air mass was adopted to analyze the role of t_a in PM₁ formation and evolution. Meanwhile, the influence of fresh emission during morning and evening rush hours was minimized by using the data observed from 10:00 to 18:00, as discussed by Qin et al. (2016) (Qin et al., 2016); and **detailed response can be found in Comment 5**. Meanwhile, more comparisons between suburban and urban chemistry have been discussed in the revised manuscript. We summarized and compared the percentage of different chemical species in PM₁ derived from many observations in summertime of Beijing in urban and suburban, as shown in Fig. R1. Typically, the fraction of OA (48.3%) in suburban Beijing is higher than that in urban (33-38%), while the contribution of SIA (51.7%) in suburban is smaller than those in urban (58-64%) (Hu et al., 2017; Huang et al., 2010; Sun et al., 2010; Sun et al., 2012). The reason may be the difference in the emissions of gaseous precursors (e.g., SO₂ and NO_x) and their conversion ratio to SIA (Hu et al., 2017; Li et al., 2020).

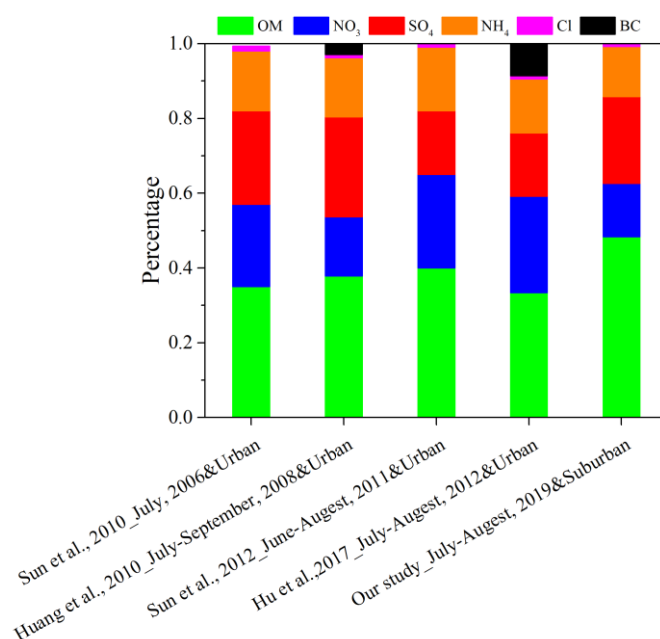


Figure R1. Comparison of percentage of different chemical species in PM₁ derived from other observations in summertime of Beijing in urban and suburban. **(This figure was added as Figure S7 in the revised SI)**

Revision in the manuscript:

Lines 241-247 (in revised version, both here and below), Add “The percentage of different chemical species in PM₁ reported in previous observations in summertime of Beijing in urban and suburban was compared in Fig. S7. Typically, the fraction of OA (48.3%) in suburban Beijing is higher than those in urban (33-38%), while the contribution of SIA (51.7%) in suburban is smaller than those in urban (58-64%) (Hu et al., 2017; Huang et al., 2010; Sun et al., 2010; Sun et al., 2012). The reason may be the difference in the emissions of gaseous precursors (e.g., SO₂ and NO_x) and their conversion ratio to SIA (Hu et al., 2017; Li et al., 2020).”

Comment 1: Section 2.1–In general, the authors are missing a lot of details here to

fully evaluate the study as well as being able to reproduce and/or to put into context of other studies. This includes and is not limited to: -What material was used for the inlet lines? Different material has different impacts on losses of the particles and gases being sampled? -What was the length and residence time for the inlet lines? -Was the same inlet line used for gases and PM or different inlet lines? -Where was the inlet line located, e.g., was it sticking out a window, on the roof? How far was it located from the building? -Where was the sample line in regards of potential sources? This includes trees/parks, parking lots, roadways, any asphalt or paint material? -Was there an impactor used for PM sampling? Was the PM dried prior to being sampled by AMS to minimize the impact of aerosol liquid water on collection efficiency? -A figure that shows the inlet and a map of where the inlet was in location of the area would help with many of these questions.

Response: Thanks for your valuable suggestion. We added all requested details in the revised manuscript and a frame figure used to describe the information of the inlet was added to the SI.

Revision in the manuscript:

Lines 104-113, Add “The aerosols and gases were sampled using a 1/4-inch stainless steel tube and 1/4-inch PFA tube, respectively, and the sampling inlet extended out of the window about 2.0 m (Fig. S1). For the aerosol sampling line, the total flow rate was adjusted to 6.0 L min^{-1} using an additional pump to reduce the residence time of aerosols ($\sim 0.7 \text{ s}$). Meanwhile, an impactor with a size cut of $2.5 \mu\text{m}$ was equipped in the front of this sampling inlet to remove coarse aerosols. A series of gas analyzers shared the

gas sampling line, and the total flow rate was about 5.5 L min^{-1} with a corresponding residence time of gas of $\sim 0.8 \text{ s}$. During the field observation period, the average temperature and RH were $28.3 \pm 3.3 \text{ }^\circ\text{C}$ ($22.1\text{-}37.7 \text{ }^\circ\text{C}$) and $62.0 \pm 17.5\%$ ($21.7\text{-}93.6\%$), respectively. The wind speed was in a range of 0.40 to 5.37 m s^{-1} with an average value of $1.62 \pm 0.93 \text{ m s}^{-1}$.”

Lines 117-119, Add “the aerosols are dried using a diffusion dryer containing silica gel before they entered the HR-ToF-AMS to minimize the impact of aerosol liquid water on collection efficiency (CE)”

Supplement, Fig. S1 had been added to the SI as follows:

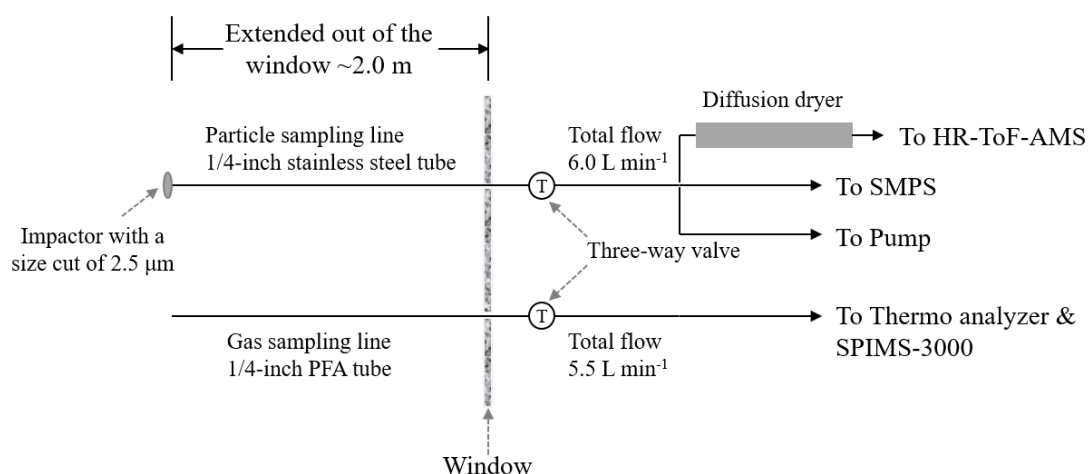


Figure S1. Detailed information of the sampling line, the corresponding flow rate, as well as the arranged instruments.

Comment 2: Section 2.2–It’s unclear if the W and V mode is used for all the analysis throughout the paper or if only one mode, please specify. -Further, to address reviewer #1 concerns and concerns I will bring up, was there a measurement of wind direction/speed?

Response: In this study, the mass concentration of NR-PM₁ was derived from V mode

considering its higher sensitivity, and the elemental ratios was obtained from W mode due to its higher resolution.

The wind speed and wind direction were also effectively recorded by Vaisala M451 during the sub-period from 2nd August to 21st August 2019, as shown in Fig. R2. During this sub-period, the wind speed was in a wide range from 0.40 to 5.37 m s⁻¹ with an average of 1.62 ± 0.93 m s⁻¹, and the dominant wind direction was southeast and south.

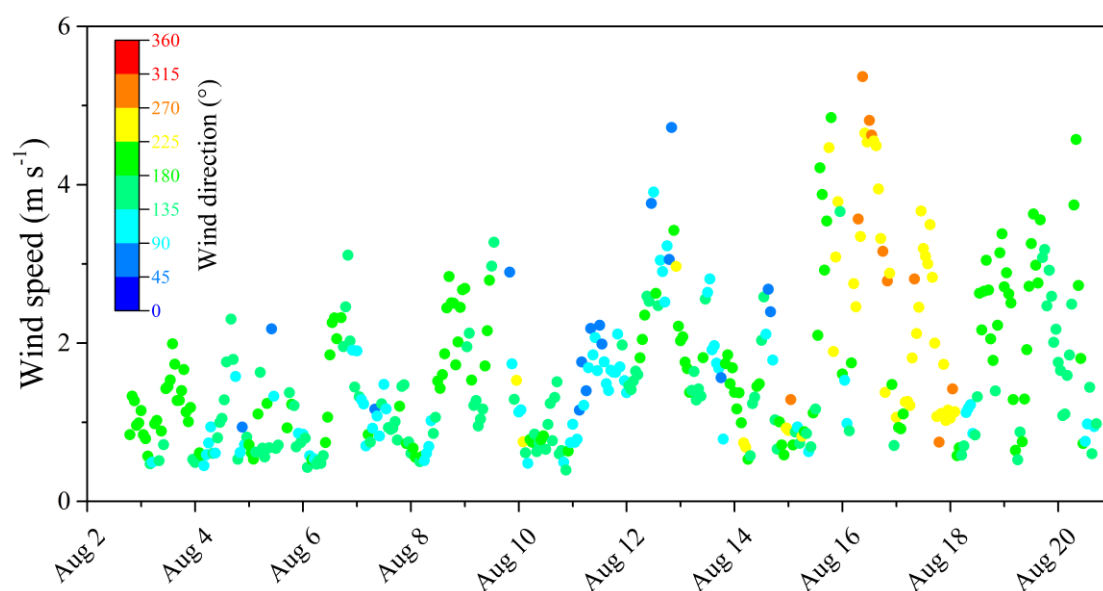


Figure R2. Time series of wind speed and wind direction from 2nd August to 21st August 2019.

Revision in the manuscript:

Lines 112-113, Add “The wind speed was in a range of 0.40 to 5.37 m s⁻¹ with an average value of 1.62 ± 0.93 m s⁻¹.”

Lines 125-126, Add “The mass concentration of NR-PM₁ was derived from V mode considering its higher sensitivity, and the elemental ratios was obtained from W mode due to its higher resolution.”

Lines 141-143, Change “In addition, two Apresys Temperature Humidity Data Loggers (179-UTH, Apresys, USA) were also used to measure the meteorological parameters including temperature (T) and RH.” **To** “In addition, the meteorological parameters including temperature (T), RH, wind speed and direction were recorded by an automatic weather station (Vaisala M451).”

Comment 3: Section 2.3.1—I appreciate the authors actually discuss the calibrations and how they determined CE. Thank you! -It is strongly recommended in the AMS community to not include charge with ammonium, sulfate, nitrate, and chloride, as some portion of the signal is from organic material (therefore it can not be stated directly that it is an inorganic compound with a charge).

Response: Thanks for your suggestion. The statement of charged inorganic compounds have been corrected in the revised manuscript.

Lines 148-149, Change “In order to obtain the quantitative mass concentrations of different species (i.e., OA, SO₄²⁻, NO₃⁻, NH₄⁺, and Cl⁻)” **To** “In order to obtain the quantitative mass concentrations of different species (i.e., OA, SO₄, NO₃, NH₄, and Cl)”

Comment 4: Section 2.3.2—The PMF analysis currently as presented is not convincing, which impacts some of the conclusions of this paper. -First, it is generally recommended to use the "semi-volatile" when the factor coincides with a thermodenuder measurement, as "semi-volatile" is meaningless without measuring whether the components of OA actually volatilize at low vs high temperatures. -Second, looking at the SI material, there

is not enough evidence/evaluation of the PMF solutions to be convinced the current solution are actually separate factor or splits of a factor. The "LO-OOA" factor is missing a comparison. All factors should have the r or R^2 of the time series. LO-OOA and MO-OOA look similar and that LO-OOA may be a noisier version of MO-OOA. If the authors at least compare the spectra with published spectra, that provide more evidence of the solutions selected here.

Response: Thanks for your suggestion. The usage of “semi-volatile OOA (SV-OOA)” has been changed to “intermediate oxidized OOA (IO-OOA)” in the revised manuscript.

In order to evaluate the credibility of current PMF solution, the correlations of all factors with the corresponding reference was also obtained, which all had higher R^2 (>0.6), as shown in Fig. R3, which had been added to the SI. Meanwhile, we compared the mass spectra of LO-OOA with the published spectra observed in Beijing (Chen et al., 2020; Hu et al., 2016), as given in Fig. R4, and they are highly correlated with a large $R^2 > 0.8$. Meanwhile, LO-OOA and MO-OOA had the distinct diurnal variation and time series ($R^2 < 0.4$, Fig. R3c), which indicated that the identification of LO-OOA is reasonable.

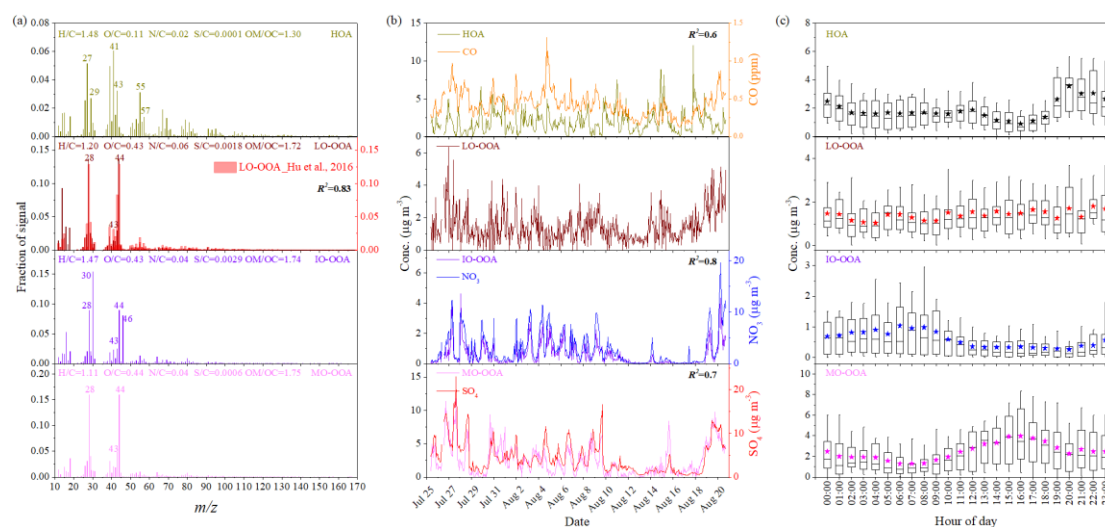


Figure R3. (a) Mass spectra, (b) time series, and (c) diurnal variation of the four factors (HOA, LO-OOA, IO-OOA and MO-OOA) identified from the PMF analysis to the HR-ToF-AMS data during the whole field observation. **(This figure was added as Figure S4 in the revised SI)**

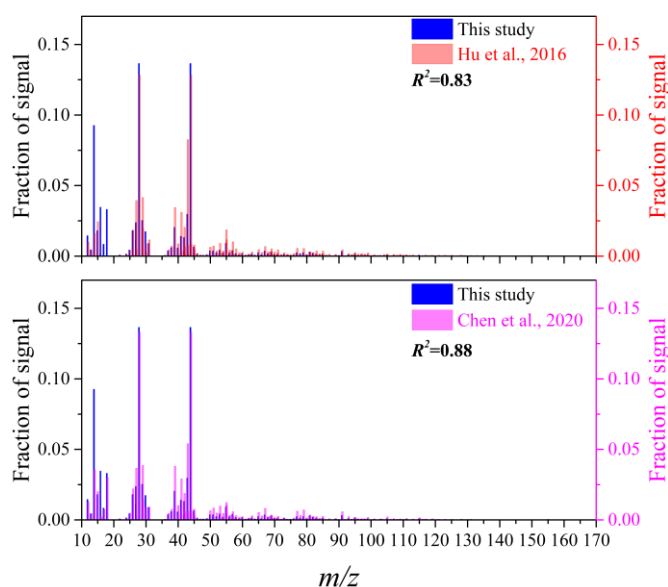


Figure R4. Comparison of mass spectra of LO-OOA identified from in this study and that published spectra observed in Beijing (Chen et al., 2020; Hu et al., 2016).

Supplement, In order to make the PMF analysis convince, more additional methodological had been supplemented to the SI as follows:

S2. PMF solutions and quality assurance

We carefully evaluated the PMF results and solution according to the procedures mentioned by Zhang et al. (2011) (Zhang et al., 2011) and Ulbrich et al. (2009) (Ulbrich et al., 2009). We determined the optimal solution of each dataset via examining their residuals of PMF fits (Fig. S3). When the number of factors increased from two to five, the value of Q/Q_{exp} was 2.038, 1.834, 1.736 and 1.699, respectively (Fig. S3i). As suggested by Ulbrich et al. (2009), a large decrease in Q/Q_{exp} indicates that the

additional factor may explain a large fraction of unaccounted variability in the data. Meanwhile, the explained fraction of the data variation increased from 97.8 % to 99.6 % with the number of factors increased from two to five (Fig. S3i).

In order to evaluate the credibility of current PMF solution, the correlations of all factors with the corresponding reference was also obtained, which all had higher R^2 (>0.6), as shown in Fig. S4. Meanwhile, we compared the mass spectra of LO-OOA with the published spectra observed in Beijing (Chen et al., 2020; Hu et al., 2016), as given in Fig. S4, and they are highly correlated with a large $R^2 > 0.8$. Meanwhile, LO-OOA and MO-OOA had the distinct diurnal variation and time series ($R^2 < 0.4$, Fig. S3c), which indicated that the identification of LO-OOA is reasonable. Based on these considerations, we concluded that the PMF solution with four factors is the optimal solutions, which exhibits the distinct time series and the corresponding mass spectrum.

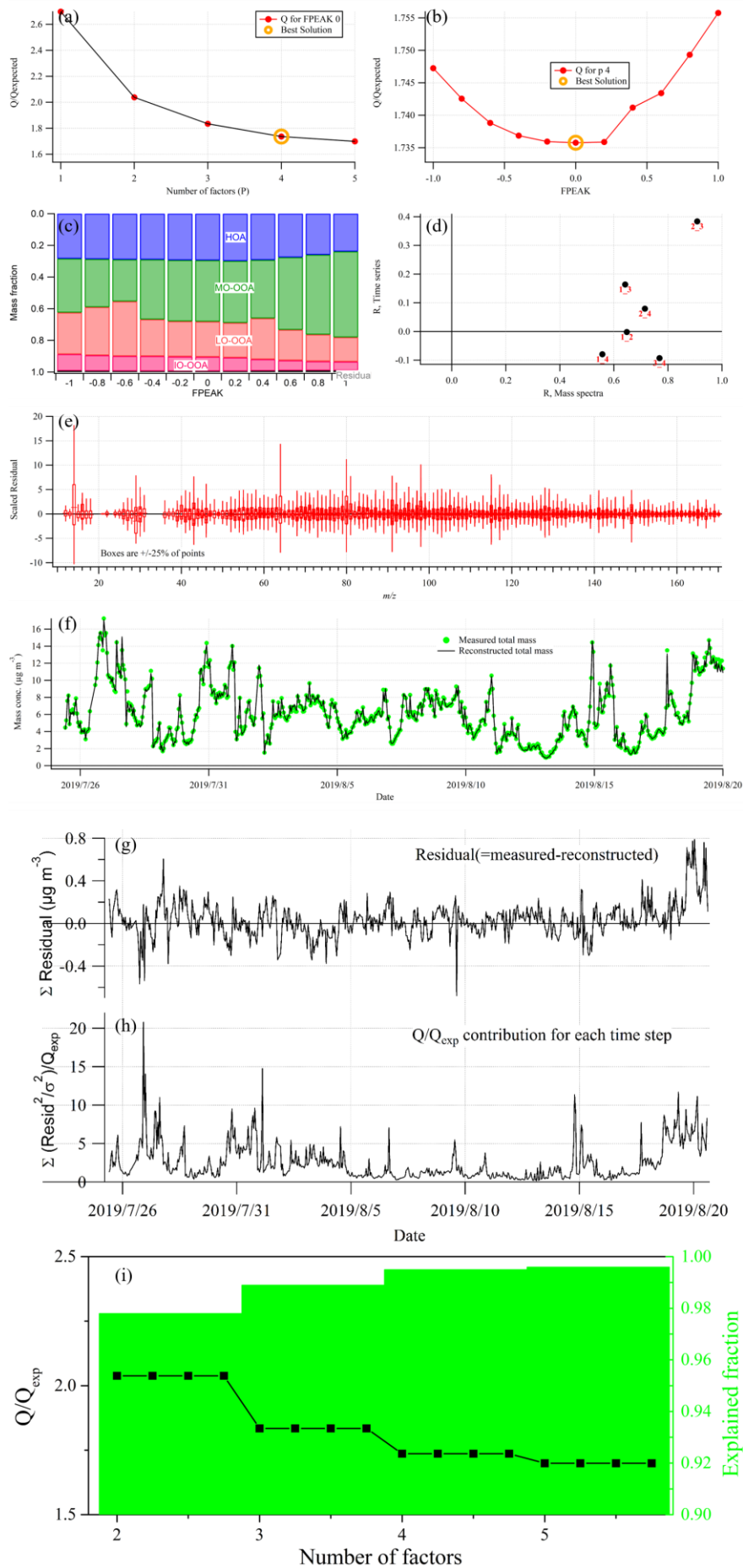


Figure S3. Summary of key diagnostic plots of the PMF results for an HR-ToF-AMS dataset acquired during this field observation: (a) Q/Q_{exp} as a function of number of factors (P) selected for PMF modeling. For the four-factor solution (i.e., the best P): (b) Q/Q_{exp} as a function of FPEAK, (c) fractions of OA factors vs. FPEAK, (d) correlations among PMF factors, (e) the box and whiskers plot showing the distributions of scaled residuals for each m/z , (f) time series of the measured organic mass and the reconstructed organic mass (= HOA + LO-OOA + IO-OOA + MO-OOA), (g) variations of the residual (= measured – reconstructed) of the fit, (h) the Q/Q_{exp} for each point in time, (i) the changes of Q/Q_{exp} and the explained variation from two-factor to five-factor solutions.

Comment 5: Section 2.3.3–Reviewer #1 has mentioned many concerns about this that I agree need to be addressed. Other things to consider: -The authors are trying to differentiate urban and suburban chemistry and use an OH value for urban Beijing, where OH may be very different. Also, the use of this value can make it hard to compare against prior studies. Instead of making any assumptions, I would recommend using a value of 1.5×10^6 molec./cm³ OH, which allows for direct comparisons with prior studies. -I agree that the emission ratio of 3.3 is hard to discern from the SI figure. I recommend that authors to use the methods from de Gouw et al., JGR, 2017, where they looked at the ratios at nighttime, which removes the impact of photochemistry and boundary layer dilution on the emission ratio. -The time series in the SI strongly suggests different emission sources/airmasses being sampled during the period (e.g.,

Aug 4 where Benzene > Toluene). Use of wind speed/direction may give insight about the sources of the air being sampled and allow for better calculation of photochemical age. -The very old ages (>12 hrs) is very surprising as that has not been typically observed in most other urban SOA studies (including many urban studies that assume a much lower OH concentration). It could be due to (1) not including impact of dilution, (2) mixing different airmasses/sources, and/or (3) using toluene: benzene ratio. Toluene: benzene ratio is typically suggested for older air masses as trimethylbenzene is more sensitive to younger ages (Parrish et al., JGR, 2007). More investigation into the cause of these older ages would be of value. -Are the authors using all data (day & night) or only day time? Interpretation of night time data in regards to photochemical age can be challenging and misleading.

Response: Thanks for your suggestion. According to the suggestion of Reviewer #1, 72 h back trajectories have been performed using the NOAA-HYSPLIT4 (HYbrid Single-Particle Lagrangian Integrated Trajectory) model (Draxier and Hess, 1998). Four times for each day, 00:00, 06:00, 12:00 and 18:00 UTC, terminating in a height of 50 m, and 112 trajectories were calculated and then used to do the air mass cluster analysis. A total of 4 backward-trajectory clusters were identified (Clusters 1-4, Fig. R5), which indicated that more than half (Cluster 2, 64%) of the observation period is dominated by the southern air mass.

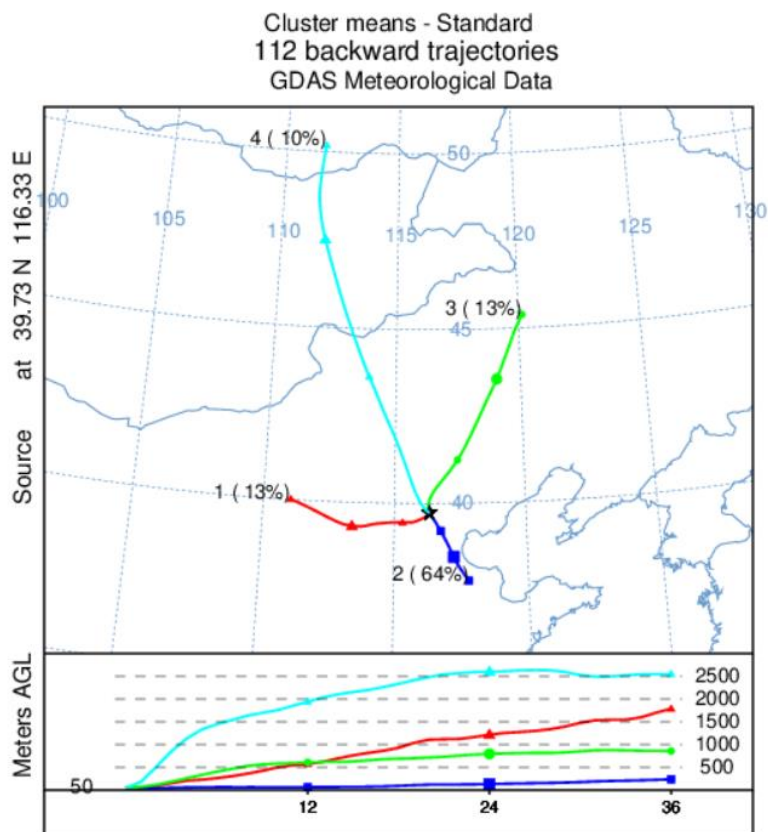


Figure R5. Mean back trajectories for 4 trajectory clusters arriving at Beijing Institute of Petrochemical Technology (BIPT) from different height. **(This figure was added as Figure S5 in the revised SI)**

To improve the reliability of photochemical age (t_a) as the surrogates of atmospheric oxidation capacity, the observation period included by Cluster 2 was adopted, which had the similar emission sources. Meanwhile, the influence of fresh emission during morning and evening rush hours was minimized by using the data observed from 10:00 to 18:00, as discussed by Qin et al. (2016) (Qin et al., 2016). In order to better compare with other studies, the OH concentration has been assumed as 1.5×10^6 molecule cm^{-3} in the revised manuscript. Meanwhile, the emission concentration ratio of toluene and benzene has been estimated to be 2.71 ± 0.39 ppb ppb⁻¹ (Fig. R6) according to the methods described by de Gouw et al. (2017) (de Gouw

et al., 2017), where the ratios at nighttime was used to remove the impact of photochemistry and boundary layer dilution on the emission ratio. This ratio is slightly higher than the value that calculated from the emission ratio of toluene and benzene (~2.2) in Beijing (Yuan et al., 2012), which might be related to the extensive utilization of solvents containing toluene for painting and printing in Daxing District, Beijing (Yuan et al., 2010). Uncertainties in estimating the initial emission ratio of toluene to benzene do exist and the influence to the analysis was discussed by Yuan et al. (2012), and they estimated that the uncertainties of the emission ratios were less than 50%. The concentration ratio of toluene and benzene during this observation period (i.e. Cluster 2) was given in Fig. R6. During this observation period, the average ratio of toluene to benzene is about 1.18, which is consistent with previous studies in Beijing (Liu et al., 2017; Wang et al., 2016; Wang et al., 2012).

As for the very old ages (>12 h), larger photochemical age also observed during the previous observations in China, such as nearly 30 h in the winter of Zhejiang in 2011 (Peng et al., 2016), and up to 72 h in the winter of Beijing in 2018 (Chu et al., 2021). All these were estimated using the similar method and the assumed OH concentration (i.e., 1.5×10^6 molecule cm^{-3}). Meanwhile, these larger photochemical ages might be due to the extremely high OH concentration with the maximum up to 1.3×10^7 molecule cm^{-3} during this field observation (Fig. R6). The OH concentration ([OH]) can be calculated using the following an empirical power-law function. Such a strong relation between OH and $J(\text{O}^1\text{D})$ can also be retrieved from the results of previous field observations (Rohrer and Berresheim, 2006; Berresheim et al., 2003;

Brauers et al., 2001; Holland et al., 1998; Gu et al., 2020; Holland et al., 2003).

$$[\text{OH}] = a \times (J(\text{O}^1\text{D}) / 10^{-5} \text{ s}^{-1})^b + c$$

where the coefficients of $a = 2.0 \times 10^6 \text{ molecule cm}^{-3}$, $b = 1$, $c = 0.43 \times 10^6 \text{ molecule cm}^{-3}$, which were proposed by Holland et al. (2003) for urban areas. $J(\text{O}^1\text{D})$ was the photolysis frequencies of O_3 , which can be estimated according to the measured $J(\text{NO}_2)$.

In this study, t_a presented a higher level at noon, which followed a similar diurnal variation of estimated OH concentration, as shown in Fig. R6.

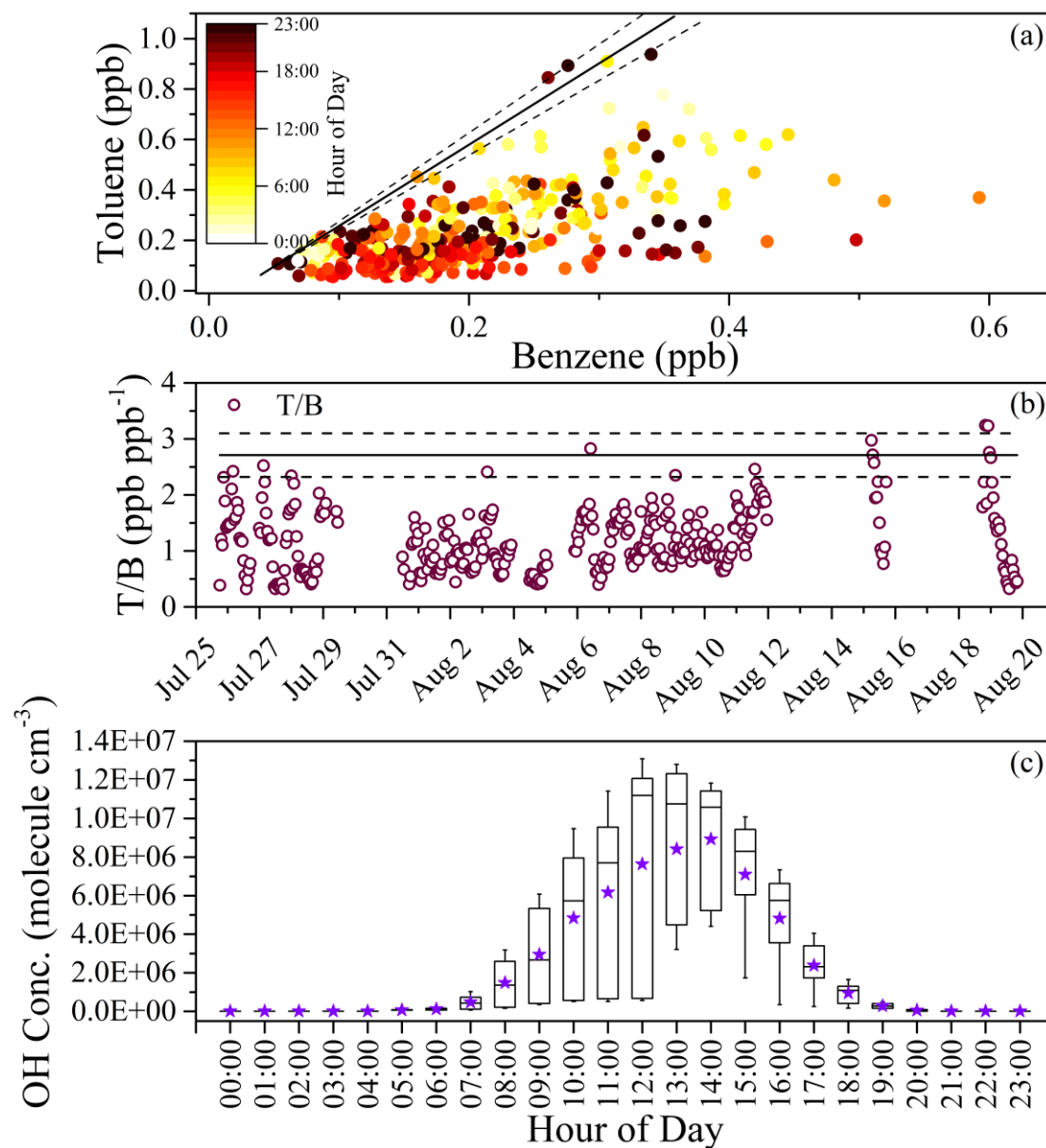


Figure R6. (a) Determination of the emission ratio of toluene vs. benzene. The scatter plot of toluene vs. benzene color-coded by the time of day, (b) Time series of concentration ratio of benzene and toluene, (c) diurnal variation of estimated OH concentration during the observation period included by Cluster 2.

Revision in the manuscript:

Section 2.3.3 Photochemical age had been rewritten in the revised manuscript as follows:

In this study, the equivalent photochemical age (t_a) was calculated to characterize the OH exposure dose of the air mass, as expressed in the following equation. This method had been widely used to provide useful information on the photochemical process in the atmosphere (Yuan et al., 2012; Parrish et al., 2007; de Gouw et al., 2005; McKeen et al., 1996).

$$t_a = \frac{1}{[\text{OH}](k_{\text{toluene}} - k_{\text{benzene}})} \times \left[\ln\left(\frac{[\text{toluene}]}{[\text{benzene}]}\right)_0 - \ln\left(\frac{[\text{toluene}]}{[\text{benzene}]}\right) \right]$$

where [OH] is the average OH concentration in the ambient air and is assumed as 1.5×10^6 molecule cm^{-3} in order to better compare with other studies (Mao et al., 2009; Chu et al., 2016; Liu et al., 2018). k_{toluene} and k_{benzene} are the rate constants for the reactions of OH with toluene (5.63×10^{-12} cm^3 molecule $^{-1}$ s $^{-1}$) and benzene (1.22×10^{-12} cm^3 molecule $^{-1}$ s $^{-1}$), respectively (Atkinson and Arey, 2003). $\left(\frac{[\text{toluene}]}{[\text{benzene}]}\right)_0$ is the emission concentration ratio of toluene and benzene before aging in the atmosphere, and was determined to be 2.71 ± 0.39 (Fig. S6, in the Supplement) according to the methods described by de Gouw et al. (2017), where the ratio at nighttime was used to

avoid the impact of photochemistry and boundary layer dilution on the emission ratio.

$\frac{[\text{toluene}]}{[\text{benzene}]}$ is the measured concentration ratio of toluene and benzene, as given in Fig.

S6. Based on the back trajectories and air mass cluster analysis (Draxier and Hess, 1998) (Details can be found in SI), an observation period (Cluster 2, Fig. S5) with the similar emission sources was adopted. Furthermore, the data observed from 10:00 to 18:00 was used to minimize the influence of fresh emission during morning and evening rush hours on t_a , as discussed by Qin et al. (2016). In this study, t_a was determined to be in the range of 4-90 h, which is comparable to previous studies (up to 72 h) conducted in China (Peng et al., 2016; Chu et al., 2021). Meanwhile, t_a had a higher level at noon, which is similar to the diurnal trend of OH radicals observed in summertime of Beijing (Tan et al., 2019).

Supplement, Details of back trajectories analysis have been added to the SI as follows:

S3. Back trajectories analysis

72 h back trajectories have been performed using the NOAA-HYSPLIT4 (HYbrid Single-Particle Lagrangian Integrated Trajectory) model (Draxier and Hess, 1998). Four times for each day, 00:00, 06:00, 12:00 and 18:00 UTC, terminating in a height of 50 m, and 112 trajectories were calculated and used to do the air mass cluster analysis. A total of 4 backward-trajectory clusters were identified (Clusters 1-4, Fig. S5), which indicated that more than half (Cluster 2, 64%) of the observation period is dominated by the southern air mass. This observation period included by Cluster 2 was adopted to analyze the role of t_a in PM_{10} formation and evolution.

Comment 6: Section 3.1 The sentences leading up to the sentence in line 214/215 ("With further improvement in air quality, PM₁ concentration would decrease in the future. Then, the contribution of OA in PM₁ is likely to increase.") currently do not support this. The logic is hard to follow, especially as other factors could influence PM₁, including meteorology (boundary layer height, RH, and temperature have confounding impacts as well as wind direction/speed = source) and specific emission controls as certain controls might have different overall impacts on the precursors, OH concentration, etc that leads to the observed PM₁.

Response: We agree with the reviewer that there are many factors, mainly including meteorology factors and emission controls, will significantly affect PM₁ concentration. Meteorology factors are constantly changing during the field observations, which makes it difficult to identify the factors affecting PM₁ concentration in isolation. In terms of control policy, the "Beautiful China" strategy has been launched by the Chinese government in 2020, which requires that all cities in China attain 35 $\mu\text{g m}^{-3}$ or below for annual mean concentration of PM_{2.5} by 2035 (Xing et al., 2020). Therefore, PM₁ concentration would also decrease in the future. SO₂, NO_x, NH₃, and VOCs are the key precursors of secondary PM_{2.5}. As the crucial precursors of OA, VOCs are derived from a wealth of sources, as well as lack effective control methods relative to other precursors. The relative change in emissions of these precursors had also been estimated to be -62% for SO₂, -17% for NO_x, +11% for NMVOCs, and +1% for NH₃ during the period of 2010-2017 (Zheng et al., 2018). The relatively increased VOCs would lead to the increase contribution of OA in PM₁.

To make the logic clear, this sentence was revised as follows:

Lines 444-449, Add “VOCs, as the crucial precursors of SOA, are derived from a wealth of sources, as well as lack effective control methods relative to other precursors. Meanwhile, the relative change in emissions of VOCs had also been estimated to be increased +11%, while other precursors (mainly SO₂) decreased during the period of 2010-2017 (Zheng et al., 2018). The relatively increased VOCs would lead to the increase contribution of SOA in PM₁.”

Comment 7: Section 3.2 By itself, the section is not fully convincing, in large part due to the concerns about photochemical ages discussed above and in Reviewer #1. Some other analysis that can be done to improve the section and to be able to compare to other studies is to look at the OOA vs O_x (e.g., Herndon et al., GRL, 2008; Wood et al., ACP, 2010; Hayes et al., JGR, 2013) and/or OA/CO vs photochemical age (e.g., de Gouw et al., JGR, 2005; Hayes et al., JGR, 2013). Both analysis would take dilution and other processes out of the impacts observed.

Response: Thanks for your valuable suggestion. In order to evaluate the effect of the photochemical aging process, the observation period with the similar emission sources was adopted, which was determined by the back trajectories as mentioned above. Meanwhile, in order to minimize the influence of fresh emission during morning and evening rush hours, according to Qin et al. (2016), we set the time range from 10:00-18:00 for discussing the photochemical age. When examining the photochemical evolution of each species, a more intuitive method as suggested by Reviewer #1 was

used, which is to group species concentration based on photochemical age. Additionally, raw data of each species concentration has been presented in the revised figures.

The time series of total OOA (=LO-OOA + IO-OOA + MO-OOA) and O_x (=O₃+NO₂) was compared and both of them presented similar temporal changes ($R^2 = 0.85$, Fig. R7a). As shown in Fig. R7b, the regression slope for OOA vs. O_x was also determined to be $0.130 \pm 0.002 \mu\text{g m}^{-3} \text{ ppb}^{-1}$, which was slightly lower than those observed in Pasadena ($0.146 \pm 0.001 \mu\text{g m}^{-3} \text{ ppb}^{-1}$) (Hayes et al., 2013), Riverside, CA ($0.142 \pm 0.004 \mu\text{g m}^{-3} \text{ ppb}^{-1}$) (Docherty et al., 2011) and Mexico City ($0.156 \pm 0.001 \mu\text{g m}^{-3} \text{ ppb}^{-1}$) (Aiken et al., 2009). This might be related to the observed high concentrations of light alkenes during this period. These species will cause high O₃ concentrations but will not contribute greatly to the formation of SOA. The scatter data are colored by the time of day, and the slope observed in the morning is steeper than that in the afternoon, which was also observed in other field measurements, and has been attributed to several factors including increased evaporation of SV-OOA, mixing with air aloft that contains residual OOA and O_x during boundary layer growth, and OOA production occurring on shorter timescales than O_x (Hayes et al., 2013; Herndon et al., 2008; Wood et al., 2010).

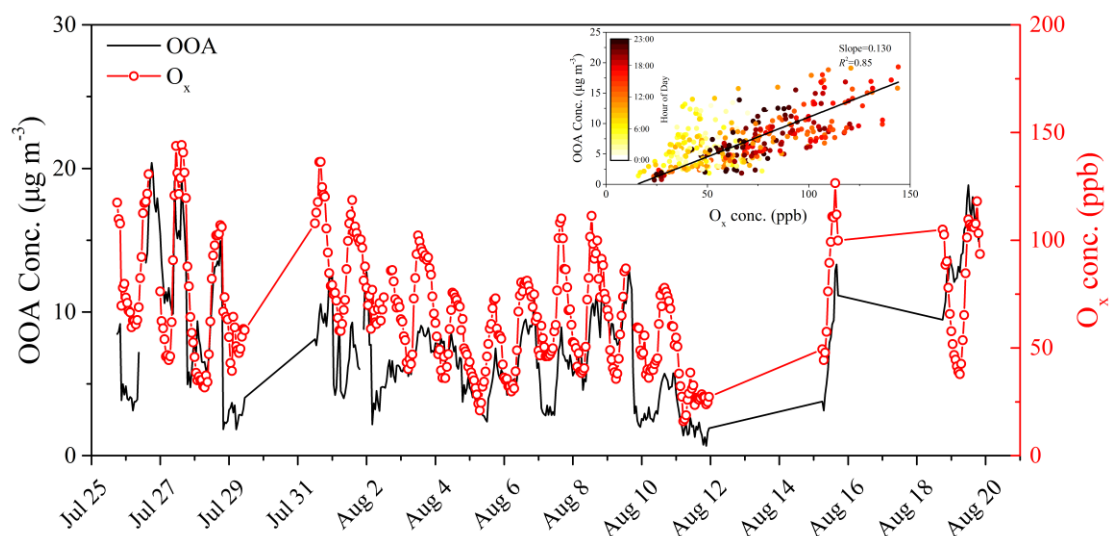


Figure R7. Time series of OOA (=LO-OOA + IO-OOA + MO-OOA) and O_x ($=O_3 + NO_2$). Inset: Scatter plot of OOA vs. O_x with linear fit and colored by the time of day. The regression slope is 0.130 ($R^2 = 0.85$). **(This figure was added as Figure 3 in the revised manuscript)**

The evolution of $OA/\Delta CO$ as a function of photochemical age was also presented in Fig. R8, in which ΔCO was obtained by the measured CO concentrations subtracting its background concentration, and the latter was determined to be 0.1 ppm according to the method described by DeCarlo et al. (2010) (DeCarlo et al., 2010). As shown in Fig. R8, the concentration ratio of organic and OOA (especially for MO-OOA) to ΔCO also increased significantly with t_a , which could be attributed to the SOA formation from the photochemical process and also similar to the evolution trend of the ratios of OA components to HOA with t_a (Fig. 3).

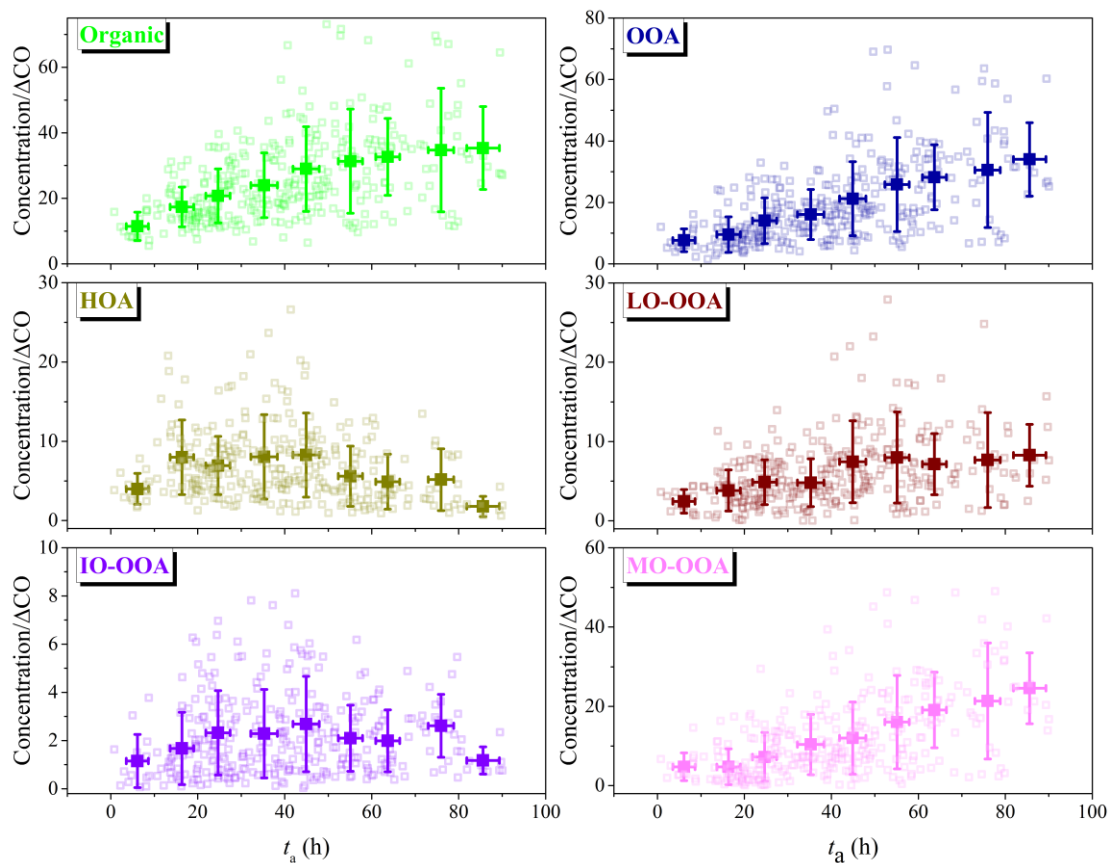


Figure R8. The evolution of OA/ Δ CO vs. photochemical age. The data are binned according to the value of t_a (10 h increment). **(This figure was added as Figure S14 in the revised SI)**

Revision in the manuscript:

Lines 269-271, Change: “In order to evaluate the effect of the photochemical aging process on PM₁ concentrations, the relationships among t_a , O_x, OA concentration, and binned PM₁ concentration were analyzed and shown in Fig. 2. Both t_a and O_x simultaneously rose with the increasing concentration of PM₁. This suggested that the photochemical aging process was closely related to the PM pollution level, and that the photochemical process becomes more intensive with the increase of VOCs and O_x at higher PM₁ concentrations. In addition, the similar evolutionary trends of t_a and O_x during this summertime observation further confirmed that they are closely correlated.”

to “In order to evaluate the effect of the photochemical aging process, the relationships between O_x , PM_{10} , OA concentration and binned t_a were analyzed and shown in Fig. 2. These species concentration all increase positively with the increasing of t_a .”

Lines 288-298, Add: “The time series of total OOA (=LO-OOA + IO-OOA + MO-OOA) and O_x was also compared (Fig. 3) and they presented similar temporal changes ($R^2 = 0.85$). As shown in the inset of Fig. 3, the regression slope for OOA vs. O_x was determined to be $0.130 \pm 0.002 \mu\text{g m}^{-3} \text{ ppb}^{-1}$, which was slightly lower than those observed in Pasadena ($0.146 \pm 0.001 \mu\text{g m}^{-3} \text{ ppb}^{-1}$) (Hayes et al., 2013), Riverside, CA ($0.142 \pm 0.004 \mu\text{g m}^{-3} \text{ ppb}^{-1}$) (Docherty et al., 2011) and Mexico City ($0.156 \pm 0.001 \mu\text{g m}^{-3} \text{ ppb}^{-1}$) (Aiken et al., 2009). This might be related to the observed high concentrations of light alkenes during this period. These species will cause high O_3 concentrations but will not contribute greatly to the formation of SOA. The scatter data are colored by the time of day, and the slope observed in the morning is steeper than that in the afternoon, which was also observed in other field measurements, and was mainly due to the increased evaporation of IO-OOA (Hayes et al., 2013; Herndon et al., 2008; Wood et al., 2010).”

Lines 352-359, Add: “Additionally, the evolution of $OA/\Delta CO$ as a function of t_a was also presented in Fig. S14, in which ΔCO was obtained by the measured CO concentrations subtracting its background concentration, and the latter was determined to be 0.1 ppm according to the method described by DeCarlo et al. (2010) (DeCarlo et al., 2010). As shown in Fig. S14, the concentration ratio of organic and OOA (especially for MO-OOA) to ΔCO also increased significantly with t_a , which could be attributed to

the SOA formation from the photochemical process and also similar to the evolution trend of the ratios of OA components to HOA with t_a (Fig. 4). These results further indicated the positive role of photochemical aging process in aerosol formation.”

Figures 2-3 had been modified in the revised manuscript as follows:

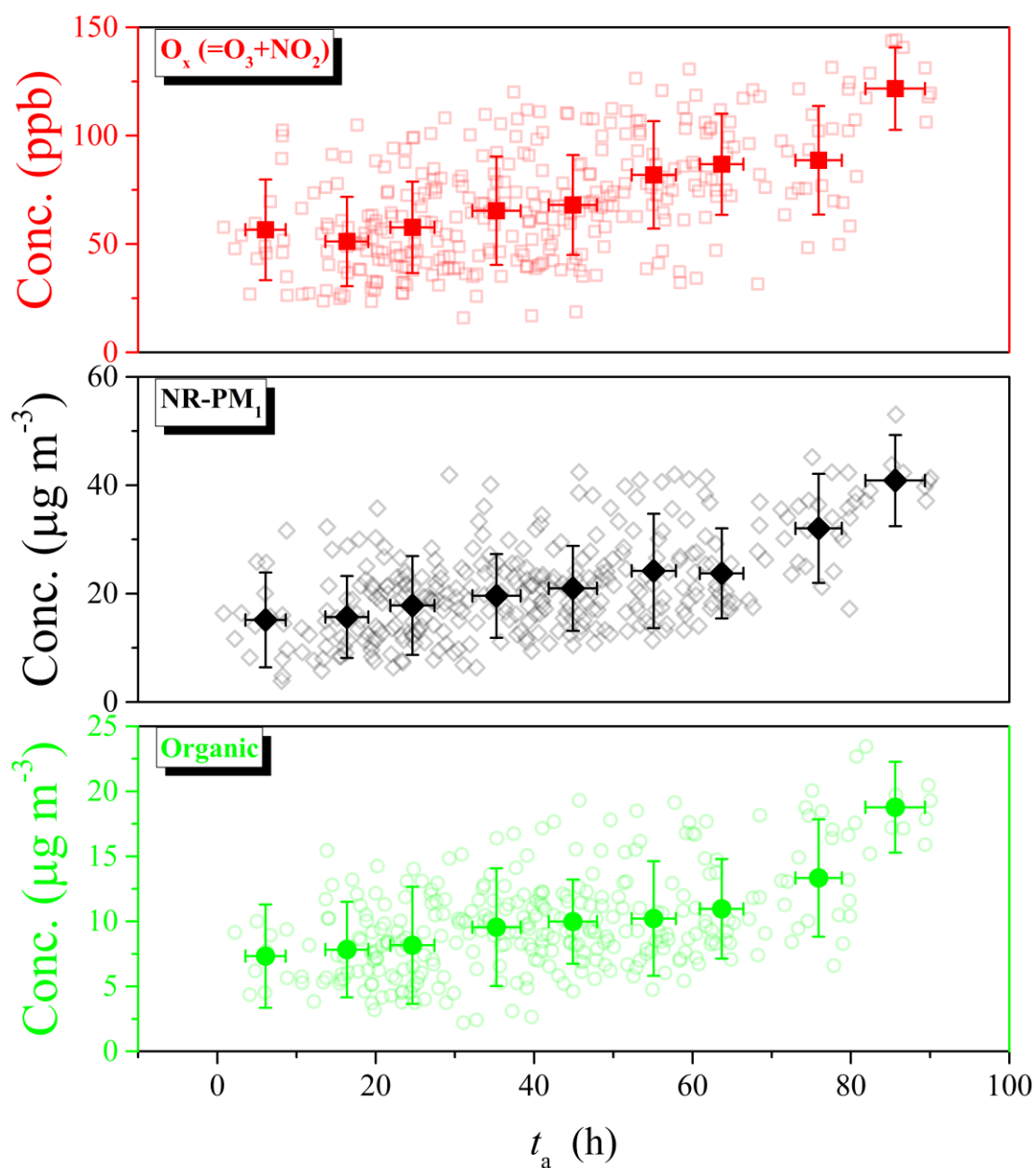


Figure 2. Relationship between photochemical age (t_a) and total oxidant (O_x), NR-PM₁ concentration, as well as organic concentration during the observation period included by cluster 2. The data are binned according to the value of t_a (10 h increment).

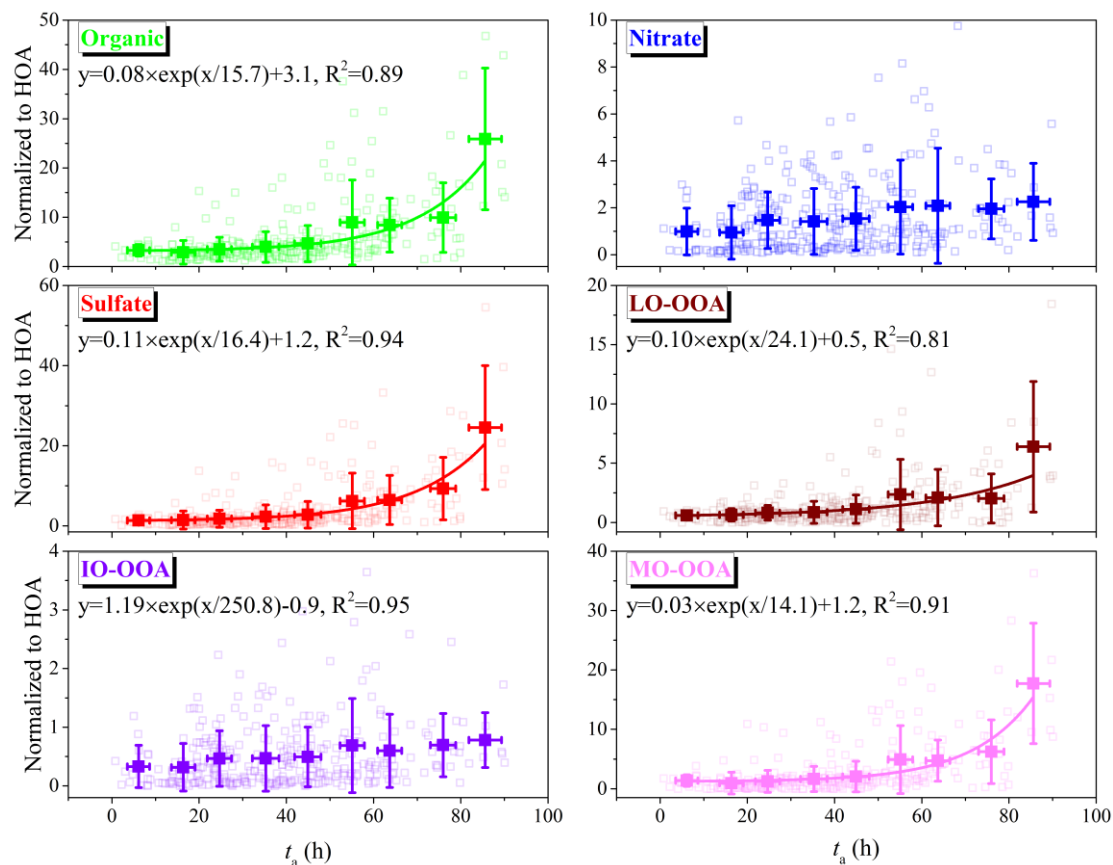


Figure 4. Variations of the ratios of mass concentrations of NR-PM₁ species and OA factors to HOA as a function of t_a . The data are binned according to the value of t_a (10 h increment). The solid lines are the results of exponential fitting with the function of $y = A \times \exp(x/B) + C$.

Comment 8: Fig. 2—The figure by itself is not convincing as there can be a lot of scatter within each value that is binned. The figures suggested above would help to understand the potential scatter or not. Also, the figure in of itself is not very convincing for the overarching story trying to be discussed here. Further, it's surprising that O_x is continuously going up with increasing PM₁ as at a certain level, PM₁ should be decreasing O_x due to less photochemistry. How much of the observations shown here are from day time vs night time?

Response: According to the above suggestion, the concentration of each species was grouped based on photochemical age, and the raw data of each species concentration has been presented in the revised manuscript. The scatter plot of O_x , NR- PM_{10} , and organic concentration also presented an increasing trend as t_a increased. This figure gives an overview information for the effect of the photochemical aging process on gas phase total oxidant and particle phase NR- PM_{10} . These species concentration all positively rose with the increasing of t_a , which suggested that the pollution level was closely related to the photochemical aging process.

The view of increased PM_{10} concentration will lead to the decreasing of O_3 was mainly based on the mechanism that heterogeneous HO_2 radical will loss on aerosol, and then suppressing O_3 formation (Li et al., 2019). However, this view has been questioned by Tan et al. (2020) (Tan et al., 2020). They analyzed the measured free radical budget and showed that the uptake of HO_2 aerosol did not impact radical chemistry. Therefore, they claimed that there was insufficient evidence to prove the significant impact of heterogeneous chemistry on radical concentrations (Tan et al., 2020). During this field observation, we found that the concentration of O_x and NR- PM_{10} all positively rose with the increasing of t_a , which indicated that both of them were homologous. Meanwhile, the time series of total OOA (i.e., SOA, the predominant species in NR- PM_{10}) and O_x also presented similar temporal changes ($R^2 = 0.85$, Fig. R7), which further supported that NR- PM_{10} traced well with O_x during this summertime observation.

In the revised manuscript, in order to minimize the influence of fresh emission

during morning and evening rush hours, we set the time range from 10:00-18:00 for discussing the photochemical age according to Qin et al. (2016) (Qin et al., 2016).

Revision in the manuscript:

Figure 2 had been modified in the revised manuscript as follows:

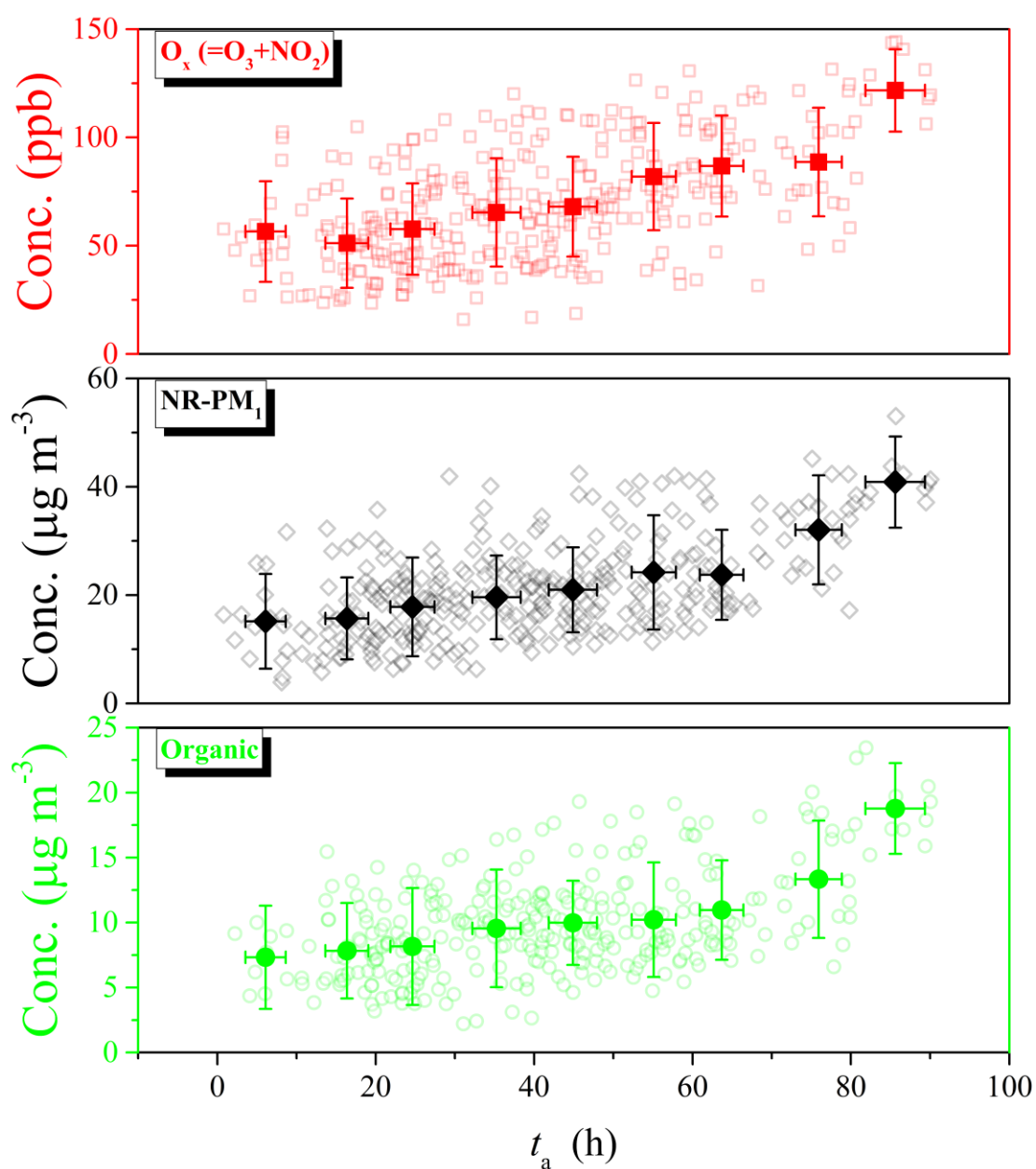


Figure 2. Relationship between photochemical age (t_a) and total oxidant (O_x), NR- PM_{10} concentration, as well as organic concentration during the observation period included by cluster 2. The data are binned according to the value of t_a (10 h increment).

Comment 9: Fig. 3—The fitting for some of the PM₁ components here is surprising, as they are not produced through photochemistry (e.g., NH₄ and Cl). Similar to Fig. 2, what does the scatter look like? Also, as NR-PM₁ is being largely controlled by SO₄ & OA, not sure that it's needed to be shown here.

Response: According to the above suggestion, raw data of each species has been presented in the form of scatter plot in the revised manuscript. The scatter plot of these species also presented an increasing trend as t_a increased.

We agree with the reviewer that ammonium (NH₄) and chloride (Cl) are not produced through photochemistry. In order to avoid this misunderstanding, the variations of the ratios of mass concentrations of NH₄, Cl, and NR-PM₁ to HOA as a function of t_a had been removed from Fig. 3, and the discussion on the relationship between NH₄ and Cl and photochemical age had been removed in the revised manuscript.

Revision in the manuscript:

Figure 3 had been modified in the revised manuscript as follows:

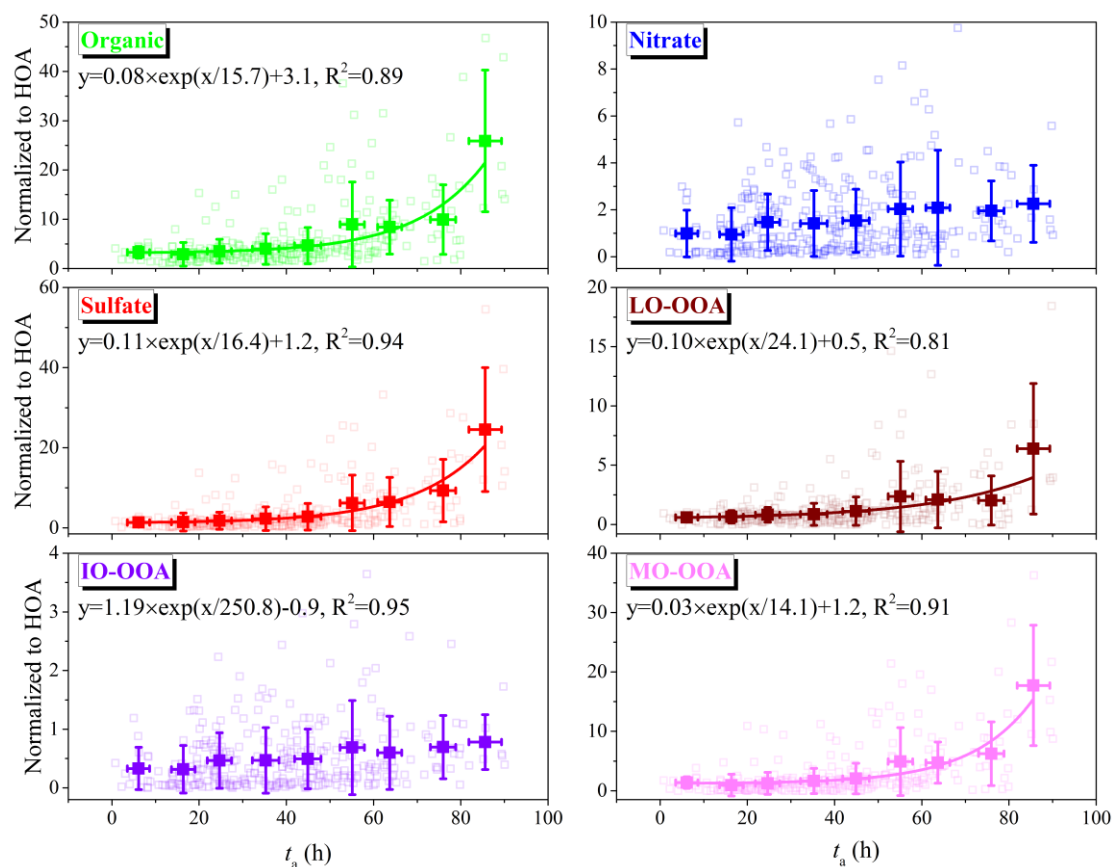


Figure 4. Variations of the ratios of mass concentrations of NR-PM₁ species and OA factors to HOA as a function of t_a . The data are binned according to the value of t_a (10 h increment). The solid lines are the results of exponential fitting with the function of $y = A \times \exp(x/B) + C$.

Comment 10: Line 295 - 298—It is erroneous to say that NH₄ mainly exists in the form of ammonium sulfate without calculating in a thermodynamic model (e.g., Pye et al., ACP, 2020). Though the measurement may show $2 \times \text{NH}_4 \text{ mol} = \text{SO}_4 \text{ mol}$, it may actually be a combination of ammonium sulfate and ammonium bisulfate that depends on temperature, aerosol liquid water, and ammonia partitioning that is not directly related to the AMS measurement. I strongly suggest removing or softening this language (here and other parts of the manuscript).

Response: Thanks for your valuable suggestion. We agree with the reviewer that the existence form of NH_4 was related to many factors. This sentence had been deleted in the revised manuscript.

Revision in the manuscript:

Lines 295-298, Delete: “The similar evolution trends of NH_4^+ and SO_4^{2-} suggested that NH_4^+ mainly existed in the form of $(\text{NH}_4)_2\text{SO}_4$ (apart from NH_4NO_3 and NH_4Cl), which could be supported by the relative contributions of these SIA species during this field observation (see Section 3.1).”

Comment 11: Section 3.3 and Fig 5–N/C and S/C ratios are typically not reported for V mode and only reported for W mode due to signal-to-noise issues, especially for the fitting of organic compounds in the V mode that contain nitrogen and/or sulfur. Were only the W mode used here or both? If both, I would recommend W only analysis or to compare W only vs W + V to see if there is a systematic difference. This noise in the fitting could also explain line 362-365 where there was no discernable change in these ratios with age.

Response: Thanks for your comment. We agree with the reviewer that N/C and S/C ratios are typically only reported from W mode. Indeed, all elemental ratios (including H/C, O/C, N/C, and S/C) were determined from W mode in our present study.

Although N-containing and S-containing organics are potentially important in the ambient air (Farmer et al., 2010), their concentration were relatively low, which was at the level of dozens to hundreds ng m^{-3} (Huang et al., 2019; Meade et al., 2016), this

might be the main reason why there was no obvious change in N/C and S/C with photochemical age. Despite this, the slight increase trend of N/C and S/C with the increase in t_a still can be observed as shown in the revised Fig. 6. These indicated that the formation of N-containing and S-containing organics was related to the photochemical process, which is consistent with the fact that both of them are the important products of gas-phase oxidation of VOCs and have also been detected in SOA (Farmer et al., 2010).

Revision in the manuscript:

Lines 393-394, Add: “All these elemental ratios were determined from W mode due to its higher resolution.”

Lines 404-406, Change “which is consistent with previous smog chamber simulations in the laboratory (Chen et al., 2019c,d)” **to:** “which is consistent with the fact that both of them are the important products of gas-phase oxidation of VOCs and have also been detected in SOA (Farmer et al., 2010; Chen et al., 2019c, d)”

Figure 5 had been modified in the revised manuscript as follows:

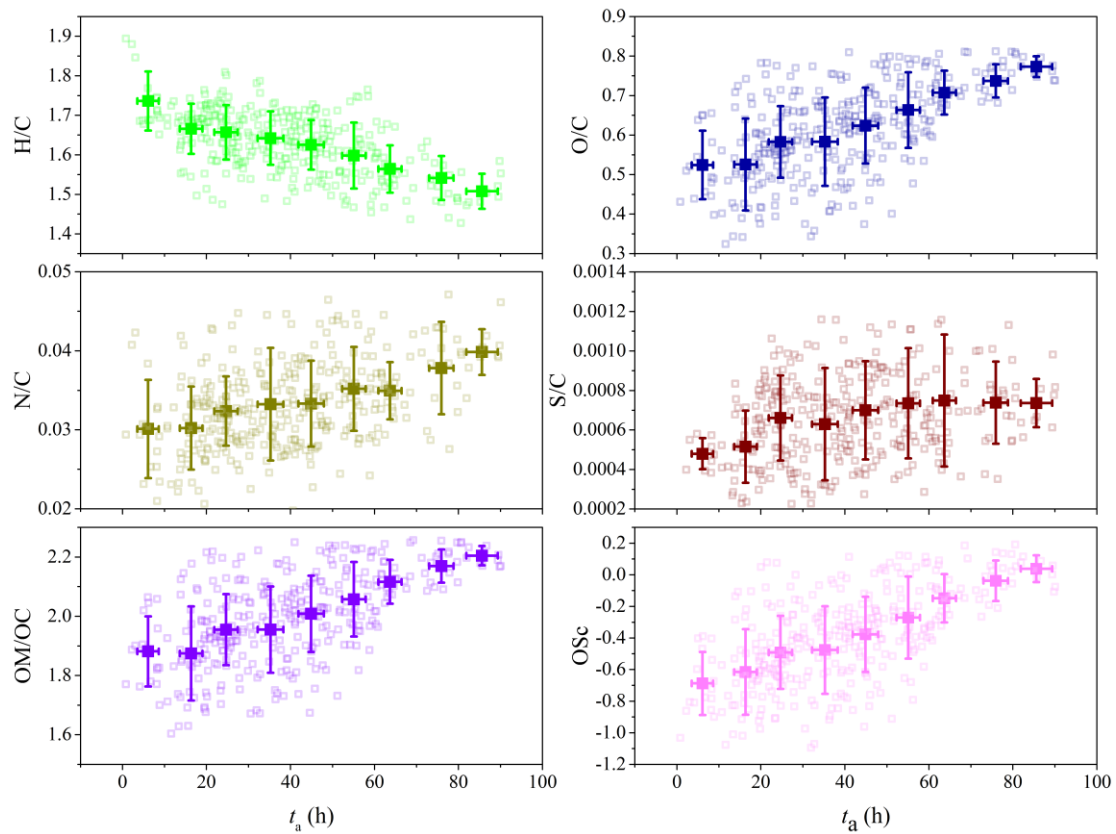


Figure 6. Variations of H/C, O/C, N/C, S/C, OM/OC and OSc as a function of t_a . The data are binned according to the value of t_a (10 h increment).

Comment 12: Fig 6–The oxidation state lines (-1, -0.5, 0, etc.) should be expanded to +/-2 for completeness

Response: The oxidation state lines had been expanded to +/-2 in the revised manuscript.

Revision in the manuscript:

Figure 6 had been modified in the revised manuscript as follows:

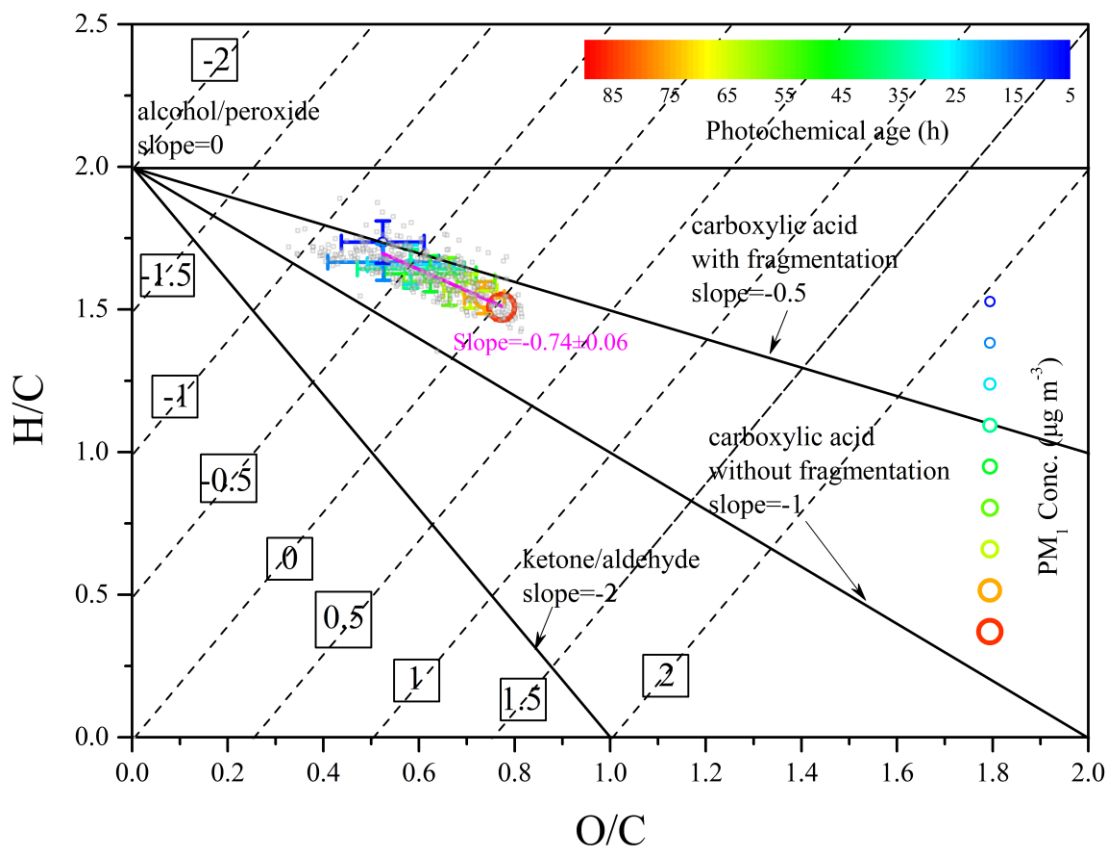


Figure 7. Van Krevelen diagram during this field observation. The data are binned according to the value of t_a (10 h increment) and color coded by t_a . The elemental composition of OA was fitted with a slope of -0.74 ($R^2 = 0.95$).

Comment 13: Line 403-406 This conclusion is misleading with the recent studies that have come out discussing the importance of non-transportation emissions of VOCs and how they dominate the photochemistry of urban environments, including from heating, cooking, and volatile chemical products. Though transportation is an important source, the authors need to at minimum recognize and discuss these important sources (see first minor comment below).

Response: Thanks for your comment. The discussions related to the importance of VOCs emitted from the non-transportation sources have been supplemented in the

revised manuscript.

Revision in the manuscript:

Lines 451-455, Add: “Meanwhile, more attention should be paid to the non-transportation sources, including heating (Cheng et al., 2018), cooking (Wang et al., 2018), asphalt-related (Khare et al., 2020), and volatile chemical products (McDonald et al., 2018), which have been reported to be non-negligible contributors to ambient VOCs, and played a dominate role in the photochemistry of urban environments, especially for SOA formation.”

Comment 14: line 254-255: Though temperature has an impact on biogenics, it also impacts many anthropogenic emissions (e.g., Pusede et al., ACP, 2014), including paint (e.g., McDonald et al., Science, 2018) and asphalt (Khare et al., Science Advances, 2020). Both need to be stated an discussed.

Response: The positive impact of temperature on the emission of anthropogenic sources, including paint and asphalt also been discussed in the revised manuscript.

Revision in the manuscript:

Lines 274-276, Change “One reason is that high temperature observed at elevated t_a levels (Fig. S6) increases the emission rates of biogenic VOCs (Fu et al., 2010)” **To** “The possible reason is that high temperature in summer can volatilize more VOCs from biogenic sources (Fu et al., 2010) and anthropogenic sources (Pusede et al., 2014) (such as paint (McDonald et al., 2018) and asphalt (Khare et al., 2020))”

Comment 15: Line 331-333–It has generally been found and considered lower NO₃ at higher photochemical age is due to dilution and evaporation of ammonium nitrate (e.g., DeCarlo et al., ACP, 2008; Nault et al., ACP, 2018).

Response: We agree with the reviewer. These two reasons have also been considered in the revised manuscript.

Revision in the manuscript:

Lines 372-373, Add “as well as the dilution effects and evaporation of ammonium nitrate (DeCarlo et al., 2008; Nault et al., 2018)”

Comment 16: Line 340 - 343–I am unsure where the numbers come from. If I try to relate the numbers listed here vs the numbers shown in Fig. 4, they do not match.

Response: These two numbers were calculated from the sum of the percentage of LO-OOA, IO-OOA, and MO-OOA in OA. They represent the relative contribution of total OOA (=LO-OOA + IO-OOA + MO-OOA) in OA.

Comment 17: Line 346 - 347–There are too many confounding factors to discuss the relationship between HOA and photochemical age, including dilution and evaporation. Either these need to be included or the sentence needs to be changed.

Response: Thanks for your comment. We agree with the reviewer that HOA was affected by many confounding factors, including dilution and evaporation. As given in Fig. R9, lower HOA concentration tended to be observed at high temperature conditions and/or in the afternoon with the higher planetary boundary layer (PBL). These factors

had been discussed and included in the revised manuscript.

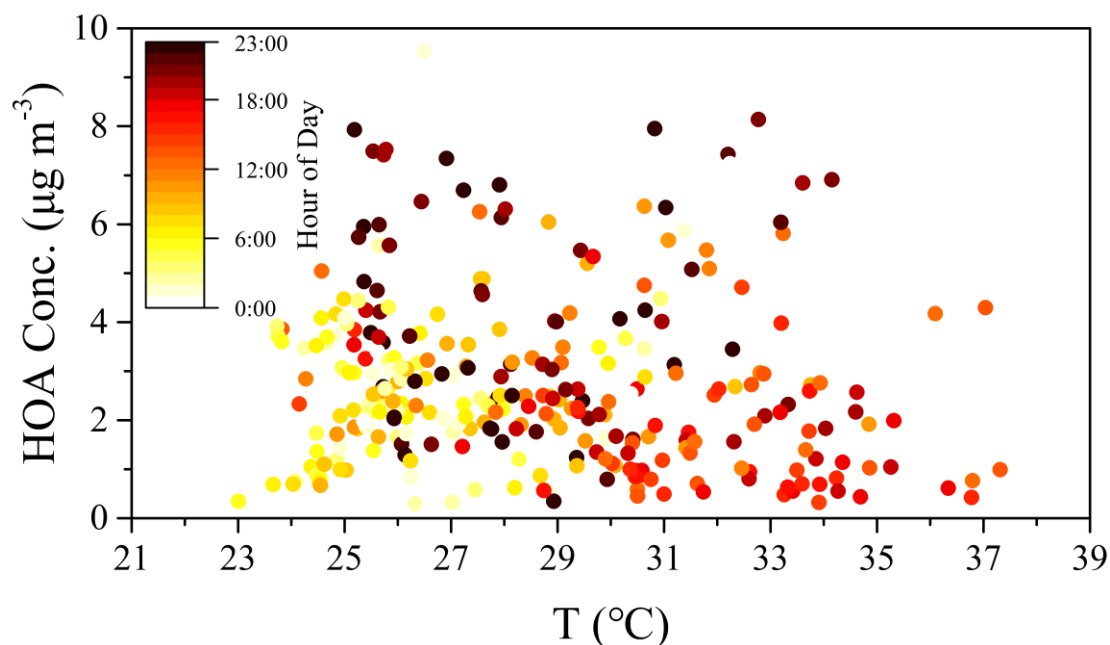


Figure R9. Scatter plot of HOA concentration and temperature. The scatter data are colored by the time of day.

Revision in the manuscript:

Lines 383-386, Add “The effects of dilution and evaporation might also be another reason for the lower HOA contribution and concentration, which tended to be observed at higher temperature conditions and/or in the afternoon with the higher planetary boundary layer (PBL) (Fig. S9)”

Comment 18: Fig. 1 y-axis for SMPS. Are the units correct

Response: As a comparison, right y axis in Fig. 1 presented the PM_{10} mass concentration derived from SMPS, which was calculated based on the volume concentration measured by SMPS and the estimated PM_{10} density. The density of PM_{10} was estimated using the following equation (Zhao et al., 2017), and the averaged density was

calculated to be 1.41 g cm^{-3} ($1.24\text{-}1.56 \text{ g cm}^{-3}$, Fig. R10a). This could be comparable with the density of atmospheric aerosols ($1.2\text{-}1.5 \text{ g cm}^{-3}$) determined in the Los Angeles Basin (Turpin and Lim, 2001; Geller et al., 2006) and also close to the recommended value of organic aerosol (1.4 g cm^{-3}) (McMurry et al., 2002; Robert et al., 2007a; Robert et al., 2007b). The time series of PM_{10} mass concentration derived from SMPS traced well with that from HR-ToF-AMS ($R^2 = 0.91$, slope = 0.95 ± 0.01 , Fig. R10b).

$$\rho_{\text{comp}} = \frac{[\text{NO}_3^-] + [\text{SO}_4^{2-}] + [\text{NH}_4^+] + [\text{Cl}^-] + [\text{Org}]}{\frac{[\text{NO}_3^-] + [\text{SO}_4^{2-}] + [\text{NH}_4^+]}{1.75} + \frac{[\text{Cl}^-]}{1.52} + \frac{[\text{Org}]}{1.2}}$$

where the densities are 1.75 g cm^{-3} for NH_4NO_3 and $(\text{NH}_4)_2\text{SO}_4$, 1.52 g cm^{-3} for NH_4Cl , and 1.2 g cm^{-3} for OA.

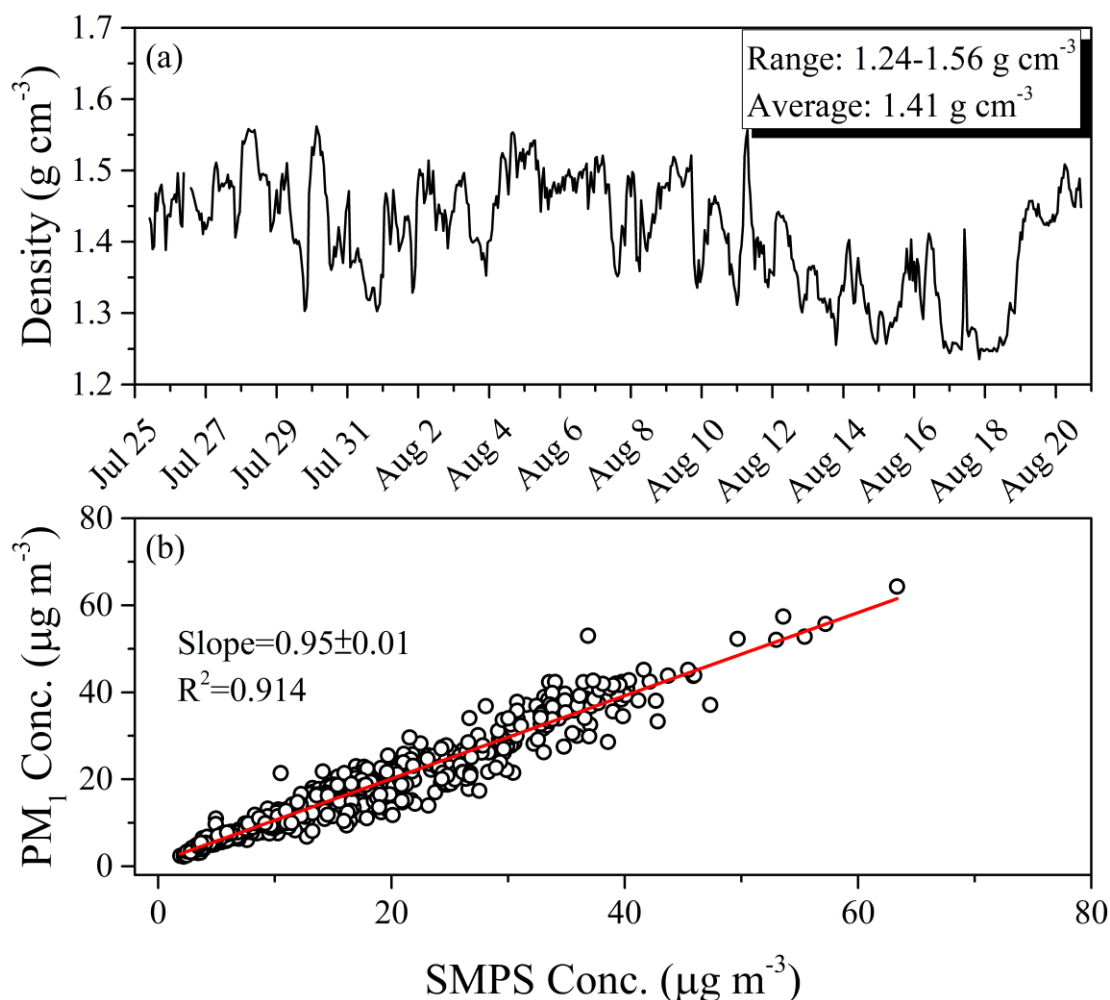


Figure R10. (a) Time series of the density of PM₁ during this field observation; (b) Relationship between PM₁ concentration derived from HR-ToF-AMS and SMPS. **(This figure was added as Figure S2 in the revised SI)**

Revision in the manuscript:

Lines 133-135, Add “PM₁ mass concentrations also calculated based on the volume concentration measured by SMPS and the estimated PM₁ density (Detailed method can be found in SI). Its time series traced well with that from HR-ToF-AMS ($R^2 = 0.91$, slope = 0.95 ± 0.01 , Fig. S2).”

Supplement, details of the method for the estimation of density have been added to the SI as follows:

S1. Method for the estimation of density

The composition-dependent density of PM₁ was estimated using the following equation (Zhao et al., 2017), and the averaged density was calculated to be 1.41 g cm⁻³ (1.24-1.56 g cm⁻³, Fig. S2). This could be comparable with the density of atmospheric aerosols (1.2-1.5 g cm⁻³) determined in the Los Angeles Basin (Turpin and Lim, 2001; Geller et al., 2006) and also close to the recommended value of organic aerosol (1.4 g cm⁻³) (McMurry et al., 2002; Robert et al., 2007a; Robert et al., 2007b).

$$\rho_{\text{comp}} = \frac{[\text{NO}_3^-] + [\text{SO}_4^{2-}] + [\text{NH}_4^+] + [\text{Cl}^-] + [\text{Org}]}{\frac{[\text{NO}_3^-] + [\text{SO}_4^{2-}] + [\text{NH}_4^+]}{1.75} + \frac{[\text{Cl}^-]}{1.52} + \frac{[\text{Org}]}{1.2}}$$

where the densities are 1.75 g cm⁻³ for NH₄NO₃ and (NH₄)₂SO₄, 1.52 g cm⁻³ for NH₄Cl, and 1.2 g cm⁻³ for OA.

References:

Aiken, A. C., Salcedo, D., Cubison, M. J., Huffman, J. A., DeCarlo, P. F., Ulbrich, I. M., Docherty, K. S., Sueper, D., Kimmel, J. R., Worsnop, D. R., Trimborn, A., Northway, M., Stone, E. A., Schauer, J. J., Volkamer, R. M., Fortner, E., de Foy, B., Wang, J., Laskin, A., Shutthanandan, V., Zheng, J., Zhang, R., Gaffney, J., Marley, N. A., Paredes-Miranda, G., Arnott, W. P., Molina, L. T., Sosa, G., and Jimenez, J. L.: Mexico City aerosol analysis during MILAGRO using high resolution aerosol mass spectrometry at the urban supersite (T0) – Part 1: Fine particle composition and organic source apportionment, *Atmos. Chem. Phys.*, 9, 6633-6653, 10.5194/acp-9-6633-2009, 2009.

Berresheim, H., Plass-Dülmer, C., Elste, T., Mihalopoulos, N., and Rohrer, F.: OH in the coastal boundary layer of Crete during MINOS: Measurements and relationship with ozone photolysis, *Atmos. Chem. Phys.*, 3, 639-649, 10.5194/acp-3-639-2003, 2003.

Brauers, T., Hausmann, M., Bister, A., Kraus, A., and Dorn, H. P.: OH radicals in the boundary layer of the Atlantic Ocean 1. Measurements by long-path laser absorption spectroscopy, *J. Geophys. Res.-Atmos.*, 106, 7399-7414, 10.1029/2000jd900679, 2001.

Chen, T., Liu, Y., Ma, Q., Chu, B., Zhang, P., Liu, C., Liu, J., and He, H.: Significant source of secondary aerosol: Formation from gasoline evaporative emissions in the presence of SO₂ and NH₃, *Atmos. Chem. Phys.*, 19, 8063-8081, 10.5194/acp-19-8063-2019, 2019a.

Chen, T., Liu, J., Liu, Y., Ma, Q., Ge, Y., Zhong, C., Jiang, H., Chu, B., Zhang, P., Ma, J., Liu, P., Wang, Y., Mu, Y., and He, H.: Chemical characterization of submicron aerosol in summertime Beijing: A case study in southern suburbs in 2018, *Chemosphere*, 247, 125918, <https://doi.org/10.1016/j.chemosphere.2020.125918>, 2020.

Chen, T. Z., Liu, Y. C., Liu, C. G., Liu, J., Chu, B. W., and He, H.: Important role of aromatic

hydrocarbons in SOA formation from unburned gasoline vapor, *Atmos. Environ.*, 201, 101-109, 10.1016/j.atmosenv.2019.01.001, 2019b.

Cheng, J., Zhang, Y., Wang, T., Xu, H., Norris, P., and Pan, W.-P.: Emission of volatile organic compounds (VOCs) during coal combustion at different heating rates, *Fuel*, 225, 554-562, <https://doi.org/10.1016/j.fuel.2018.03.185>, 2018.

Chu, B., Liu, Y., Ma, Q., Ma, J., He, H., Wang, G., Cheng, S., and Wang, X.: Distinct potential aerosol masses under different scenarios of transport at a suburban site of Beijing, *J. Environ. Sci.*, 39, 52-61, 10.1016/j.jes.2015.11.003, 2016.

Chu, B., Dada, L., Liu, Y., Yao, L., Wang, Y., Du, W., Cai, J., Dällenbach, K. R., Chen, X., Simonen, P., Zhou, Y., Deng, C., Fu, Y., Yin, R., Li, H., He, X.-C., Feng, Z., Yan, C., Kangasluoma, J., Bianchi, F., Jiang, J., Kujansuu, J., Kerminen, V.-M., Petäjä, T., He, H., and Kulmala, M.: Particle growth with photochemical age from new particle formation to haze in the winter of Beijing, China, *Sci. Total Environ.*, 753, 142207, <https://doi.org/10.1016/j.scitotenv.2020.142207>, 2021.

de Gouw, J. A., Middlebrook, A. M., Warneke, C., Goldan, P. D., Kuster, W. C., Roberts, J. M., Fehsenfeld, F. C., Worsnop, D. R., Canagaratna, M. R., Pszenny, A. A. P., Keene, W. C., Marchewka, M., Bertman, S. B., and Bates, T. S.: Budget of organic carbon in a polluted atmosphere: Results from the New England Air Quality Study in 2002, *J. Geophys. Res.*, 110, 10.1029/2004jd005623, 2005.

de Gouw, J. A., Gilman, J. B., Kim, S. W., Lerner, B. M., Isaacman-VanWertz, G., McDonald, B. C., Warneke, C., Kuster, W. C., Lefer, B. L., Griffith, S. M., Dusanter, S., Stevens, P. S., and Stutz, J.: Chemistry of Volatile Organic Compounds in the Los Angeles basin: Nighttime Removal of Alkenes and Determination of Emission Ratios, *J. Geophys. Res.-Atmos.*, 122, 11843-11861, 10.1002/2017jd027459, 2017.

DeCarlo, P. F., Dunlea, E. J., Kimmel, J. R., Aiken, A. C., Sueper, D., Crouse, J., Wennberg, P. O., Emmons, L., Shinozuka, Y., Clarke, A., Zhou, J., Tomlinson, J., Collins, D. R., Knapp, D., Weinheimer, A. J., Montzka, D. D., Campos, T., and Jimenez, J. L.: Fast airborne aerosol size and chemistry measurements above Mexico City and Central Mexico during the MILAGRO campaign, *Atmos. Chem. Phys.*, 8, 4027-4048, 10.5194/acp-8-4027-2008, 2008.

DeCarlo, P. F., Ulbrich, I. M., Crouse, J., de Foy, B., Dunlea, E. J., Aiken, A. C., Knapp, D., Weinheimer, A. J., Campos, T., Wennberg, P. O., and Jimenez, J. L.: Investigation of the sources and processing of organic aerosol over the Central Mexican Plateau from aircraft measurements during MILAGRO, *Atmos. Chem. Phys.*, 10, 5257-5280, 10.5194/acp-10-5257-2010, 2010.

Docherty, K. S., Aiken, A. C., Huffman, J. A., Ulbrich, I. M., DeCarlo, P. F., Sueper, D., Worsnop, D. R., Snyder, D. C., Peltier, R. E., Weber, R. J., Grover, B. D., Eatough, D. J., Williams, B. J., Goldstein, A. H., Ziemann, P. J., and Jimenez, J. L.: The 2005 Study of Organic Aerosols at Riverside (SOAR-1): instrumental intercomparisons and fine particle composition, *Atmos. Chem. Phys.*, 11, 12387-12420, 10.5194/acp-11-12387-2011, 2011.

Draxier, R. R., and Hess, G. D.: An overview of the HYSPLIT_4 modelling system for trajectories, dispersion and deposition, *Aust. Meteorol. Mag.*, 47, 295-308, 1998.

Farmer, D. K., Matsunaga, A., Docherty, K. S., Surratt, J. D., Seinfeld, J. H., Ziemann, P. J., and Jimenez, J. L.: Response of an aerosol mass spectrometer to organonitrates and organosulfates and implications for atmospheric chemistry, *Proc. Natl. Acad. Sci. USA*, 107, 6670-6675, 10.1073/pnas.0912340107, 2010.

Fu, P., Kawamura, K., Kanaya, Y., and Wang, Z.: Contributions of biogenic volatile organic compounds to the formation of secondary organic aerosols over Mt. Tai, Central East China, *Atmos. Environ.*, 44,

4817-4826, <https://doi.org/10.1016/j.atmosenv.2010.08.040>, 2010.

Geller, M., Biswas, S., and Sioutas, C.: Determination of particle effective density in urban environments with a differential mobility analyzer and aerosol particle mass analyzer, *Aerosol Sci. Tech.*, 40, 709-723, 10.1080/02786820600803925, 2006.

Gu, R., Zheng, P., Chen, T., Dong, C., Wang, Y. n., Liu, Y., Liu, Y., Luo, Y., Han, G., Wang, X., Zhou, X., Wang, T., Wang, W., and Xue, L.: Atmospheric nitrous acid (HONO) at a rural coastal site in North China: Seasonal variations and effects of biomass burning, *Atmos. Environ.*, 229, 117429, <https://doi.org/10.1016/j.atmosenv.2020.117429>, 2020.

Hayes, P. L., Ortega, A. M., Cubison, M. J., Froyd, K. D., Zhao, Y., Cliff, S. S., Hu, W. W., Toohey, D. W., Flynn, J. H., Lefer, B. L., Grossberg, N., Alvarez, S., Rappenglück, B., Taylor, J. W., Allan, J. D., Holloway, J. S., Gilman, J. B., Kuster, W. C., de Gouw, J. A., Massoli, P., Zhang, X., Liu, J., Weber, R. J., Corrigan, A. L., Russell, L. M., Isaacman, G., Worton, D. R., Kreisberg, N. M., Goldstein, A. H., Thalman, R., Waxman, E. M., Volkamer, R., Lin, Y. H., Surratt, J. D., Kleindienst, T. E., Offenberg, J. H., Dusanter, S., Griffith, S., Stevens, P. S., Brioude, J., Angevine, W. M., and Jimenez, J. L.: Organic aerosol composition and sources in Pasadena, California, during the 2010 CalNex campaign, *J. Geophys. Res. Atmos.*, 118, 9233-9257, <https://doi.org/10.1002/jgrd.50530>, 2013.

Herndon, S. C., Onasch, T. B., Wood, E. C., Kroll, J. H., Canagaratna, M. R., Jayne, J. T., Zavala, M. A., Knighton, W. B., Mazzoleni, C., Dubey, M. K., Ulbrich, I. M., Jimenez, J. L., Seila, R., de Gouw, J. A., de Foy, B., Fast, J., Molina, L. T., Kolb, C. E., and Worsnop, D. R.: Correlation of secondary organic aerosol with odd oxygen in Mexico City, *Geophys. Res. Lett.*, 35, <https://doi.org/10.1029/2008GL034058>, 2008.

Holland, F., Aschmutat, U., Hessling, M., Hofzumahaus, A., and Ehhalt, D. H.: Highly time resolved

measurements of OH during POPCORN using laser-induced fluorescence spectroscopy, *J Atmos Chem*, 31, 205-225, 10.1023/a:1005868520002, 1998.

Holland, F., Hofzumahaus, A., Schäfer, J., Kraus, A., and Pätz, H.-W.: Measurements of OH and HO₂ radical concentrations and photolysis frequencies during BERLIOZ, *J. Geophys. Res. Atmos.*, 108, PHO 2-1-PHO 2-23, <https://doi.org/10.1029/2001JD001393>, 2003.

Hu, W., Hu, M., Hu, W., Jimenez, J. L., Yuan, B., Chen, W., Wang, M., Wu, Y., Chen, C., Wang, Z., Peng, J., Zeng, L., and Shao, M.: Chemical composition, sources, and aging process of submicron aerosols in Beijing: Contrast between summer and winter, *J. Geophys. Res. Atmos.*, 121, 1955-1977, doi:10.1002/2015JD024020, 2016.

Hu, W., Hu, M., Hu, W. W., Zheng, J., Chen, C., Wu, Y., and Guo, S.: Seasonal variations in high time-resolved chemical compositions, sources, and evolution of atmospheric submicron aerosols in the megacity Beijing, *Atmos. Chem. Phys.*, 17, 9979-10000, 10.5194/acp-17-9979-2017, 2017.

Huang, W., Saathoff, H., Shen, X., Ramisetty, R., Leisner, T., and Mohr, C.: Chemical Characterization of Highly Functionalized Organonitrates Contributing to Night-Time Organic Aerosol Mass Loadings and Particle Growth, *Environ. Sci. Technol.*, 53, 1165-1174, 10.1021/acs.est.8b05826, 2019.

Huang, X. F., He, L. Y., Hu, M., Canagaratna, M. R., Sun, Y., Zhang, Q., Zhu, T., Xue, L., Zeng, L. W., Liu, X. G., Zhang, Y. H., Jayne, J. T., Ng, N. L., and Worsnop, D. R.: Highly time-resolved chemical characterization of atmospheric submicron particles during 2008 Beijing Olympic Games using an Aerodyne High-Resolution Aerosol Mass Spectrometer, *Atmos. Chem. Phys.*, 10, 8933-8945, 10.5194/acp-10-8933-2010, 2010.

Khare, P., Machesky, J., Soto, R., He, M., Presto, A. A., and Gentner, D. R.: Asphalt-related emissions are a major missing nontraditional source of secondary organic aerosol precursors, *Sci. Adv.*, 6, eabb9785,

10.1126/sciadv.abb9785, 2020.

Li, J., Cao, L., Gao, W., He, L., Yan, Y., Ji, D., Liu, Z., and Wang, Y.: Seasonal variations in the high time-resolved aerosol composition, sources, and chemical process of background submicron particles in North China Plain, *Atmos. Chem. Phys. Discuss.*, 2020, 1-26, 10.5194/acp-2020-213, 2020.

Li, K., Jacob, D. J., Liao, H., Shen, L., Zhang, Q., and Bates, K. H.: Anthropogenic drivers of 2013-2017 trends in summer surface ozone in China, *Proc. Natl. Acad. Sci. USA*, 116, 422-427, 10.1073/pnas.1812168116, 2019.

Liu, C., Ma, Z., Mu, Y., Liu, J., Zhang, C., Zhang, Y., Liu, P., and Zhang, H.: The levels, variation characteristics, and sources of atmospheric non-methane hydrocarbon compounds during wintertime in Beijing, China, *Atmos. Chem. Phys.*, 17, 10633-10649, 10.5194/acp-17-10633-2017, 2017.

Liu, J., Chu, B., Chen, T., Liu, C., Wang, L., Bao, X., and He, H.: Secondary organic aerosol formation from ambient air at an urban site in Beijing: effects of OH exposure and precursor concentrations, *Environ. Sci. Technol.*, 52, 6834-6841, 10.1021/acs.est.7b05701, 2018.

Mao, J., Ren, X., Brune, W. H., Olson, J. R., Crawford, J. H., Fried, A., Huey, L. G., Cohen, R. C., Heikes, B., Singh, H. B., Blake, D. R., Sachse, G. W., Diskin, G. S., Hall, S. R., and Shetter, R. E.: Airborne measurement of OH reactivity during INTEX-B, *Atmos. Chem. Phys.*, 9, 163-173, 10.5194/acp-9-163-2009, 2009.

McDonald, B. C., de Gouw, J. A., Gilman, J. B., Jathar, S. H., Akherati, A., Cappa, C. D., Jimenez, J. L., Lee-Taylor, J., Hayes, P. L., McKeen, S. A., Cui, Y. Y., Kim, S.-W., Gentner, D. R., Isaacman-VanWertz, G., Goldstein, A. H., Harley, R. A., Frost, G. J., Roberts, J. M., Ryerson, T. B., and Trainer, M.: Volatile chemical products emerging as largest petrochemical source of urban organic emissions, *Science*, 359, 760-764, 10.1126/science.aaq0524, 2018.

McKeen, S. A., and Liu, S. C.: Hydrocarbon ratios and photochemical history of air masses, *Geophys. Res. Lett.*, 20, 2363-2366, 10.1029/93gl02527, 1993.

McKeen, S. A., Liu, S. C., Hsie, E.-Y., Lin, X., Bradshaw, J. D., Smyth, S., Gregory, G. L., and Blake, D. R.: Hydrocarbon ratios during PEM-WEST A: A model perspective, *J. Geophys. Res. Atmos.*, 101, 2087-2109, 10.1029/95jd02733, 1996.

McMurry, P. H., Wang, X., Park, K., and Ehara, K.: The relationship between mass and mobility for atmospheric particles: A new technique for measuring particle density, *Aerosol Sci. Tech.*, 36, 227-238, 10.1080/027868202753504083, 2002.

Meade, L. E., Riva, M., Blomberg, M. Z., Brock, A. K., Qualters, E. M., Siejack, R. A., Ramakrishnan, K., Surratt, J. D., and Kautzman, K. E.: Seasonal variations of fine particulate organosulfates derived from biogenic and anthropogenic hydrocarbons in the mid-Atlantic United States, *Atmos. Environ.*, 145, 405-414, <https://doi.org/10.1016/j.atmosenv.2016.09.028>, 2016.

Nault, B. A., Campuzano-Jost, P., Day, D. A., Schroder, J. C., Anderson, B., Beyersdorf, A. J., Blake, D. R., Brune, W. H., Choi, Y., Corr, C. A., de Gouw, J. A., Dibb, J., DiGangi, J. P., Diskin, G. S., Fried, A., Huey, L. G., Kim, M. J., Knote, C. J., Lamb, K. D., Lee, T., Park, T., Pusede, S. E., Scheuer, E., Thornhill, K. L., Woo, J. H., and Jimenez, J. L.: Secondary organic aerosol production from local emissions dominates the organic aerosol budget over Seoul, South Korea, during KORUS-AQ, *Atmos. Chem. Phys.*, 18, 17769-17800, 10.5194/acp-18-17769-2018, 2018.

Parrish, D. D., Hahn, C. J., Williams, E. J., Norton, R. B., Fehsenfeld, F. C., Singh, H. B., Shetter, J. D., Gandrud, B. W., and Ridley, B. A.: Indications of photochemical histories of Pacific air masses from measurements of atmospheric trace species at Point Arena, California, *J. Geophys. Res. Atmos.*, 97, 15883-15901, <https://doi.org/10.1029/92JD01242>, 1992.

Parrish, D. D., Stohl, A., Forster, C., Atlas, E. L., Blake, D. R., Goldan, P. D., Kuster, W. C., and de Gouw, J. A.: Effects of mixing on evolution of hydrocarbon ratios in the troposphere, *J. Geophys. Res. Atmos.*, 112, 10.1029/2006jd007583, 2007.

Peng, J., Hu, M., Gong, Z., Tian, X., Wang, M., Zheng, J., Guo, Q., Cao, W., Lv, W., Hu, W., Wu, Z., and Guo, S.: Evolution of secondary inorganic and organic aerosols during transport: A case study at a regional receptor site, *Environ. Pollut.*, 218, 794-803, 10.1016/j.envpol.2016.08.003, 2016.

Pusede, S. E., Gentner, D. R., Wooldridge, P. J., Browne, E. C., Rollins, A. W., Min, K. E., Russell, A. R., Thomas, J., Zhang, L., Brune, W. H., Henry, S. B., DiGangi, J. P., Keutsch, F. N., Harrold, S. A., Thornton, J. A., Beaver, M. R., St. Clair, J. M., Wennberg, P. O., Sanders, J., Ren, X., VandenBoer, T. C., Markovic, M. Z., Guha, A., Weber, R., Goldstein, A. H., and Cohen, R. C.: On the temperature dependence of organic reactivity, nitrogen oxides, ozone production, and the impact of emission controls in San Joaquin Valley, California, *Atmos. Chem. Phys.*, 14, 3373-3395, 10.5194/acp-14-3373-2014, 2014.

Qin, Y. M., Li, Y. J., Wang, H., Lee, B. P. Y. L., Huang, D. D., and Chan, C. K.: Particulate matter (PM) episodes at a suburban site in Hong Kong: evolution of PM characteristics and role of photochemistry in secondary aerosol formation, *Atmos. Chem. Phys.*, 16, 14131-14145, 10.5194/acp-16-14131-2016, 2016.

Robert, M. A., Kleeman, M. J., and Jakober, C. A.: Size and composition distributions of particulate matter emissions: Part 2- Heavy-duty diesel vehicles, *J. Air Waste Manage.*, 57, 1429-1438, 10.3155/1047-3289.57.12.1429, 2007a.

Robert, M. A., VanBergen, S., Kleeman, M. J., and Jakober, C. A.: Size and composition distributions of particulate matter emissions: Part 1 - Light-duty gasoline vehicles, *J. Air Waste Manage.*, 57, 1414-1428, 10.3155/1047-3289.57.12.1414, 2007b.

Rohrer, F., and Berresheim, H.: Strong correlation between levels of tropospheric hydroxyl radicals and

solar ultraviolet radiation, *Nature*, 442, 184-187, 10.1038/nature04924, 2006.

Sun, J., Zhang, Q., Canagaratna, M. R., Zhang, Y., Ng, N. L., Sun, Y., Jayne, J. T., Zhang, X., Zhang, X., and Worsnop, D. R.: Highly time- and size-resolved characterization of submicron aerosol particles in Beijing using an Aerodyne Aerosol Mass Spectrometer, *Atmos. Environ.*, 44, 131-140, 10.1016/j.atmosenv.2009.03.020, 2010.

Sun, Y., Wang, Z., Dong, H., Yang, T., Li, J., Pan, X., Chen, P., and Jayne, J. T.: Characterization of summer organic and inorganic aerosols in Beijing, China with an Aerosol Chemical Speciation Monitor, *Atmos. Environ.*, 51, 250-259, 10.1016/j.atmosenv.2012.01.013, 2012.

Tan, Z., Lu, K., Jiang, M., Su, R., Wang, H., Lou, S., Fu, Q., Zhai, C., Tan, Q., Yue, D., Chen, D., Wang, Z., Xie, S., Zeng, L., and Zhang, Y.: Daytime atmospheric oxidation capacity in four Chinese megacities during the photochemically polluted season: a case study based on box model simulation, *Atmos. Chem. Phys.*, 19, 3493-3513, 10.5194/acp-19-3493-2019, 2019.

Tan, Z., Hofzumahaus, A., Lu, K., Brown, S. S., Holland, F., Huey, L. G., Kiendler-Scharr, A., Li, X., Liu, X., Ma, N., Min, K.-E., Rohrer, F., Shao, M., Wahner, A., Wang, Y., Wiedensohler, A., Wu, Y., Wu, Z., Zeng, L., Zhang, Y., and Fuchs, H.: No Evidence for a Significant Impact of Heterogeneous Chemistry on Radical Concentrations in the North China Plain in Summer 2014, *Environ. Sci. Technol.*, 54, 5973-5979, 10.1021/acs.est.0c00525, 2020.

Turpin, B. J., and Lim, H. J.: Species contributions to PM_{2.5} mass concentrations: Revisiting common assumptions for estimating organic mass, *Aerosol Sci. Tech.*, 35, 602-610, 10.1080/02786820152051454, 2001.

Ulbrich, I. M., Canagaratna, M. R., Zhang, Q., Worsnop, D. R., and Jimenez, J. L.: Interpretation of organic components from positive matrix factorization of aerosol mass spectrometric data, *Atmos. Chem.*

Phys., 9, 2891-2918, 10.5194/acp-9-2891-2009, 2009.

Wang, G., Cheng, S., Wei, W., Zhou, Y., Yao, S., and Zhang, H.: Characteristics and source apportionment of VOCs in the suburban area of Beijing, China, *Atmos. Pollut. Res.*, 7, 711-724, <https://doi.org/10.1016/j.apr.2016.03.006>, 2016.

Wang, H., Xiang, Z., Wang, L., Jing, S., Lou, S., Tao, S., Liu, J., Yu, M., Li, L., Lin, L., Chen, Y., Wiedensohler, A., and Chen, C.: Emissions of volatile organic compounds (VOCs) from cooking and their speciation: A case study for Shanghai with implications for China, *Sci. Total Environ.*, 621, 1300-1309, <https://doi.org/10.1016/j.scitotenv.2017.10.098>, 2018.

Wang, Y., Ren, X., Ji, D., Zhang, J., Sun, J., and Wu, F.: Characterization of volatile organic compounds in the urban area of Beijing from 2000 to 2007, *J. Environ. Sci.*, 24, 95-101, [https://doi.org/10.1016/S1001-0742\(11\)60732-8](https://doi.org/10.1016/S1001-0742(11)60732-8), 2012.

Wood, E. C., Canagaratna, M. R., Herndon, S. C., Onasch, T. B., Kolb, C. E., Worsnop, D. R., Kroll, J. H., Knighton, W. B., Seila, R., Zavala, M., Molina, L. T., DeCarlo, P. F., Jimenez, J. L., Weinheimer, A. J., Knapp, D. J., Jobson, B. T., Stutz, J., Kuster, W. C., and Williams, E. J.: Investigation of the correlation between odd oxygen and secondary organic aerosol in Mexico City and Houston, *Atmos. Chem. Phys.*, 10, 8947-8968, 10.5194/acp-10-8947-2010, 2010.

Xing, J., Lu, X., Wang, S., Wang, T., Ding, D., Yu, S., Shindell, D., Ou, Y., Morawska, L., Li, S., Ren, L., Zhang, Y., Loughlin, D., Zheng, H., Zhao, B., Liu, S., Smith, K. R., and Hao, J.: The quest for improved air quality may push China to continue its CO₂ reduction beyond the Paris Commitment, *Proc. Natl. Acad. Sci. USA*, 202013297, 10.1073/pnas.2013297117, 2020.

Yuan, B., Shao, M., Lu, S., and Wang, B.: Source profiles of volatile organic compounds associated with solvent use in Beijing, China, *Atmos. Environ.*, 44, 1919-1926, 10.1016/j.atmosenv.2010.02.014, 2010.

Yuan, B., Shao, M., de Gouw, J., Parrish, D. D., Lu, S., Wang, M., Zeng, L., Zhang, Q., Song, Y., Zhang, J., and Hu, M.: Volatile organic compounds (VOCs) in urban air: How chemistry affects the interpretation of positive matrix factorization (PMF) analysis, *J. Geophys. Res. Atmos.*, 117, 10.1029/2012jd018236, 2012.

Zhang, Q., Jimenez, J. L., Canagaratna, M. R., Ulbrich, I. M., Ng, N. L., Worsnop, D. R., and Sun, Y.: Understanding atmospheric organic aerosols via factor analysis of aerosol mass spectrometry: a review, *Anal. Bioanal. Chem.*, 401, 3045-3067, 10.1007/s00216-011-5355-y, 2011.

Zhao, J., Du, W., Zhang, Y., Wang, Q., Chen, C., Xu, W., Han, T., Wang, Y., Fu, P., Wang, Z., Li, Z., and Sun, Y.: Insights into aerosol chemistry during the 2015 China Victory Day parade: results from simultaneous measurements at ground level and 260 m in Beijing, *Atmos. Chem. Phys.*, 17, 3215-3232, 10.5194/acp-17-3215-2017, 2017.

Zheng, B., Tong, D., Li, M., Liu, F., Hong, C., Geng, G., Li, H., Li, X., Peng, L., Qi, J., Yan, L., Zhang, Y., Zhao, H., Zheng, Y., He, K., and Zhang, Q.: Trends in China's anthropogenic emissions since 2010 as the consequence of clean air actions, *Atmos. Chem. Phys.*, 18, 14095-14111, 10.5194/acp-18-14095-2018, 2018.